~~CONFIDENTIAL~~

CALIFORNIA INSTITUTE OF TECHNOLOGY

Hydrodynamics Laboratories

OPTIMUM SLENDERNESS RATIO OF A STABLE LOW-DRAG BODY

No. 55.1

A REPORT ON RESEARCH CONDUCTED UNDER CONTRACT WITH
THE OFFICE OF NAVAL RESEARCH OF THE DEPARTMENT OF THE NAVY

~~CONFIDENTIAL~~

Navy Department
OFFICE OF NAVAL RESEARCH
Contract N6onr-24428

OPTIMUM SLENDERNESS RATIO OF A STABLE LOW-DRAG BODY

by
F. Barton Brown
Research Engineer

Hydrodynamics Laboratory
California Institute of Technology
Pasadena, California

Robert T. Knapp, *Director*

September 1949

Report No. N-55.1

Copy No. 103

CONTENTS

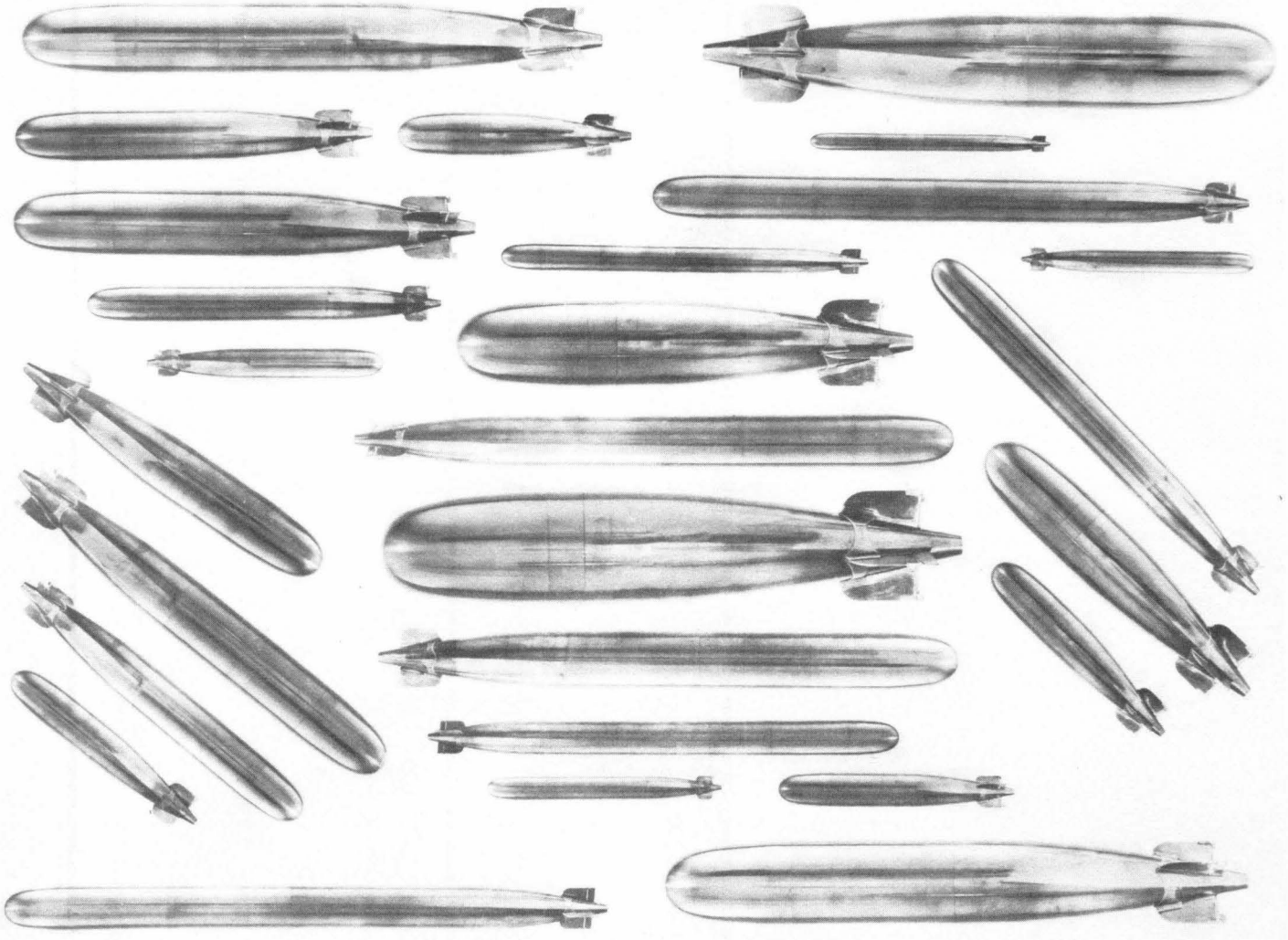

Fig. 1—Composite Group of Bodies of Various Slenderness Ratios

The nose in this group is the "halfbody," and the afterbody is from the MK 13-1 torpedo.

OPTIMUM SLENDERNESS RATIO OF A CYLINDRICAL MIDSECTION BODY

ABSTRACT

This paper presents a theoretical and experimental method of selecting the optimum slenderness ratio of a body with cylindrical midsection. Whether such a body is a large submarine or its arch enemy, the depth charge, the problem remains to find a slenderness ratio which will permit the fastest possible velocity consistent with the power or sinking weight available.

Considerable research has been done to determine the hydrodynamic characteristics of nose shapes both alone and combined with various afterbodies. In one of our reports[1*] we have pointed out that any one of several different nose shapes could be used on a particular body with little change in the total drag coefficient, and tests for certain afterbody shapes would probably bring similar results.

Due to practical considerations, most bodies have a cylindrical midsection. Therefore, a typical underwater body of axial symmetry consists of arbitrarily selected nose and afterbody shapes separated by a cylindrical midsection.

For dynamic stability, any underwater body must have fins which increase the surface area and, to some degree, the residual drag. We must necessarily consider the effect of such fins on slenderness ratio. In the following discussion of a particular concrete example, the emphasis has been placed on a body with a nose and afterbody with fins, of the same geometrical shape as the MK 13-1 torpedo (less shroud ring). The MK 13-1 torpedo is dynamically stable, has a cylindrical midsection, and has been tested with other nose shapes.[1]

After examination of the factors affecting the optimum slenderness ratio, it is found that a reasonably large variation from the theoretical optimum value will have little practical effect on the velocity of the body.

Because of practical factors involved in the design of an undersea body, it may be desirable from the designer's point of view to have a relatively large slenderness ratio. This investigation shows that as far as drag per unit volume is concerned, the designer will will pay very little, if any, penalty if he disregards the drag factor and bases his selection of slenderness ratio entirely on such items as tactical requirements of maneuverability, structural design and utilization of internal space.

*See bibliography at end of this report.

Although this investigation was carried on under the Office of Naval Research Contract N6onr-24428 in the interest of the Bureau of Ships, much of the data and method of attack was developed previously under the Bureau of Ordnance Contract NOrd 9612.

TABLE OF NOMENCLATURE

This paper uses the foot-pound (force)-second system of units. However, any consistent set of units may be used in the equations.

A = cross-sectional area at maximum cross section, sq ft

B = a constant, depending on the ~~surface area~~ VOLUME of the nose and afterbody of a body of given shape; see Eq. (7), dimensionless

C_D = total drag coefficient based on cross-sectional area, A, dimensionless

C_{DF} = residual drag coefficient based on cross-sectional area, A, dimensionless

C_F = skin friction coefficient based on cross-sectional area, A, dimensionless

C_{FP} = skin friction coefficient based on surface area, S, dimensionless

D = maximum diameter of a body with cylindrical midsection which has known nose, afterbody, and fin shape

D_0 = the maximum diameter of a particular body for which the surface area and volume of the nose, afterbody, and fin surfaces are known, ft

E = a parameter dependent on the slenderness ratio and skin friction of the body; see Eq. (26), (lb sec^2) per ft^4

F = drag force, lbs

G = a parameter dependent on the slenderness ratio and residual drag of the body; see Eq. (27), (lb sec^2) per ft^4

K = any constant

L = over-all length of the body, ft

l_a = length of the afterbody; see Fig. 4, ft

l_m = length of the cylindrical center section of the body; see Fig. 4, ft

l_n = length of body nose; see Fig. 4, ft

M = the coefficient in the residual drag equation; see Eq. (18), dimensionless

m = the exponent in the residual drag equation; see Eq. (18), dimensionless

N = the coefficient in the flat plate skin friction equation; see Eq. (15), dimensionless

n = the exponent in the flat plate skin friction equation; see Eq. (15), dimensionless

P = power, ft-lbs per sec

P_H = power, horsepower

Q = a constant depending on the surface area of the nose, afterbody, and fins of a body of given shape; see Eq. (4), dimensionless

R_e = vL/ν = Reynolds number based on over-all length of body, dimensionless

R_v = $vV^{1/3}/\nu$ = Reynolds number based on volume of body, dimensionless

S = total surface area of body, ft^2

S_0 = surface area of the body's nose, afterbody, and fin surfaces for a given diameter D_0, ft^2

V = volume, ft^3

V_0 = the total volume of the nose and afterbody for a given diameter, D_0, ft^3

v = velocity, ft per sec

γ_b = specific weight of the body, lbs per ft^3

γ_f = ρg = specific weight of fluid, lbs per ft^3

$\Delta\gamma$ = $\gamma_b - \gamma_f$ = negative buoyancy, lbs per ft^3

η = over-all efficiency, per cent

ν = kinematic viscosity, ft^2 per sec

ρ = mass density of fluid, (lb sec^2) per ft^4

ψ = L/D = slenderness ratio, dimensionless

OPTIMUM BODY SHAPE

There are four hydrodynamic considerations in the determination of an optimum body shape: nose shape, afterbody shape, fin design and slenderness ratio, L/D. In one of our reports[1], we have shown that any one of several different nose shapes could be used with little change in the total drag coefficient (see Figs. 2 and 3). Also, minor variations in the afterbody shape would probably cause little change. However, hydrodynamic considerations must be reconciled with the practical aspects involved in the design and use of an underwater body. For a depth charge the following must be included: weight of explosive and propellant charge, dynamic stability in air and water, favorable cavitation characteristics, and maximum velocity consistent with the sinking weight of the body.

Some of the practical factors involved in the design of a submarine include the following: sufficient space for machinery and personnel, dynamic stability, maneuverability, freedom from cavitation, strength of hull, and maximum velocity consistent with available power.

The hydrodynamic characteristics are known for many bodies of different nose and afterbody shapes, but there is little or no information on the effect of changing the slenderness ratio. To simplify this problem, let us consider that the slenderness ratio is changed by varying the length of the cylindrical midsection of a body for which the hydrodynamic characteristics are known for some particular slenderness ratio.

RESISTANCE OF AN UNDERWATER BODY

The force required to drive any underwater body can be predicted by model studies. In the case of ships where resistance is due to wave, eddy, and frictional resistance, analysis is made by the Froude method. Here the wave resistance is a function of Froude's number, and eddy and frictional resistance a function of Reynolds number.

For an underwater body such as a torpedo (if submergence is assumed sufficient to eliminate any wave effect) the resistance of the body will be due to eddy and frictional resistance only. Therefore, Froude's number does not enter as a parameter.

If we apply Froude's method to an underwater body, we assume that the total resistance is equal to the sum of two separable parts—the frictional resistance and the residual resistance. Also by Froude's method, we can calculate the frictional resistance of the body from the resistance of a flat plate.[2,3] Therefore, knowing the total drag resistance from water tunnel tests and the frictional resistance from calculation based on available data (Schoenherr),[3] the residual resistance can be determined. As Froude's number is not a parameter, the residual resistance will be a function of Reynolds number only.

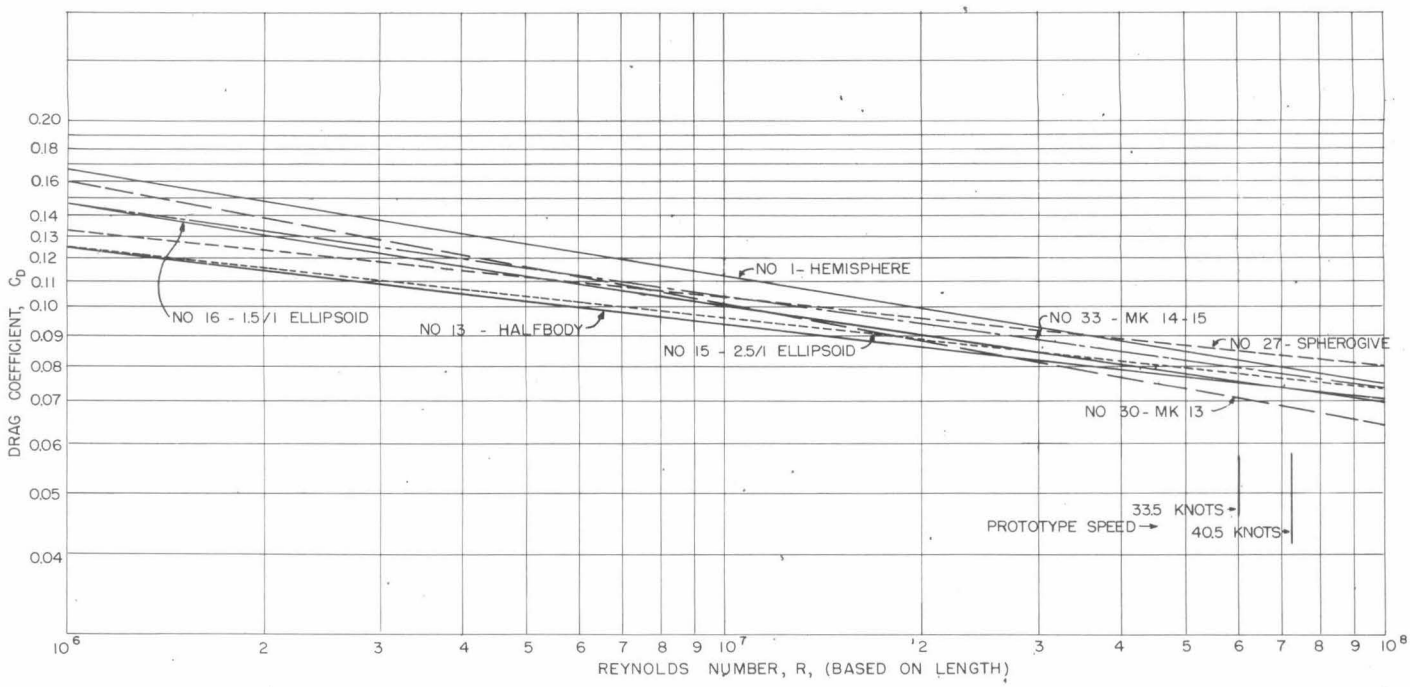

Fig. 2—Drag vs. Reynolds Number For Various Noses

The noses are shown in Fig. 3. In all runs the afterbody was the MK 13-1 torpedo shape and the slenderness ratio was 7.18.

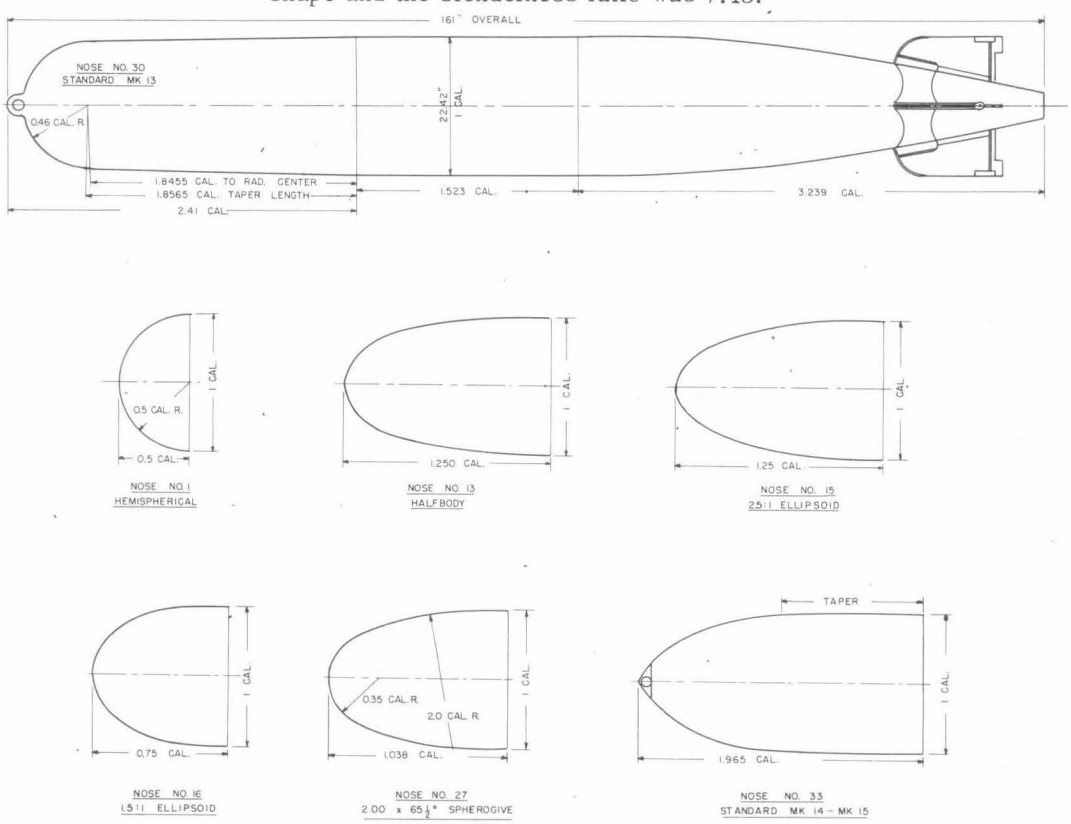

Fig. 3—Various Noses Used With MK 13-1 Torpedo Afterbody

See Fig. 2 for the resulting drag vs. Reynolds number runs.

ANALYTICAL DETERMINATION OF THE EFFECT OF CHANGE OF SLENDERNESS RATIO

Our problem is to find the effect of the slenderness ratio on the maximum velocity of an undersea body which has a given driving force and displacement. Under these conditions, the velocity depends on the hydrodynamic resistance. This resistance is made up of two factors, the skin friction and the residual drag. The problem therefore reduces to expressing these two factors as functions of the slenderness ratio. As we are considering a body with cylindrical midsection, it will be a simple matter to express the volume and surface area as functions of the slenderness ratio, a surface parameter, and a volume parameter. It follows that we can also express the skin friction and residual drag in terms of these same parameters.

Now, by adding these two expressions, we have the total drag coefficient of the body in terms of the slenderness ratio and the shape parameter. An expression for the total drag coefficient can also be written involving the velocity and frontal area of the body and the acting force. Therefore, with these two simultaneous equations, the total drag coefficient can be eliminated, and we have the desired relation between the velocity of the body, the force acting on the body, the volume of the body, and the slenderness ratio.

VOLUME AND SURFACE AREA IN TERMS OF THE SLENDERNESS RATIO

Fig. 4 shows a hypothetical body shape for which it is assumed that the proportions of nose, afterbody and tail fins are already established. The slenderness ratio can be changed only by varying the length, l_m, of the cylindrical midsection.

In the following development there are some tedious mathematical manipulations. The ratio, L/D, is awkward to handle and it is more convenient to substitute a single parameter for the slenderness ratio.

Thus,

$$\psi = L/D \tag{1}$$

From Fig. 4

$$l_m/D = \psi - (l_n + l_a)/D \tag{2}$$

The surface of the body in Fig. 4 is

$$S = [(S_0/\pi D_0^2) + \psi - (l_n + l_a)/D]\,\pi D^2 \tag{3}$$

Let

$$Q = (S_0/\pi D_0^2) - (l_n + l_a)/D \tag{4}$$

or

$$S = (Q + \psi)\pi D^2 \tag{5}$$

The volume of the body in Fig. 4 is

$$V = [(4V_0/\pi D_0^3) + \psi - (l_n + l_a)/D]\,\pi D^3/4 \tag{6}$$

Let

$$B = (4V_0/\pi D_0^3) - (l_n + l_a)/D \tag{7}$$

or

$$V = (B + \psi)\pi D^3/4 \tag{8}$$

To aid in the development of equations to follow, it is now convenient to express the reciprocal of the diameter and length in terms of the slenderness ratio and volume. From Eq. (8)

$$\frac{1}{D} = \left[\frac{\pi(B+\psi)}{4V}\right]^{1/3} \tag{9}$$

From Eq. (1) and Eq. (9)

$$\frac{1}{L} = \frac{1}{\psi}\left[\frac{\pi(B+\psi)}{4V}\right]^{1/3} \tag{10}$$

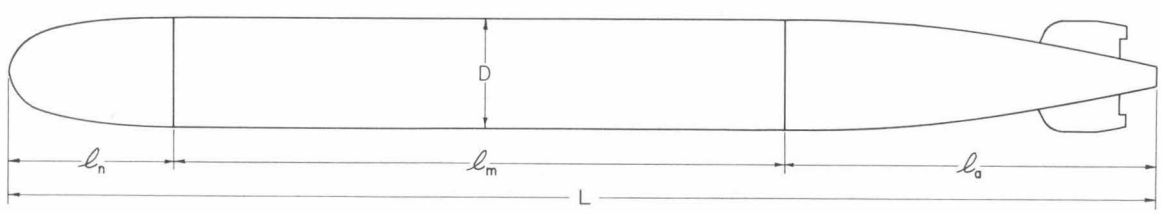

Fig. 4—Hypothetical Body With Cylindrical Midsection.

SKIN FRICTION OF THE BODY

Using Froude's method, let us assume that the flow in the boundary layer is turbulent and that the skin friction of the body can be calculated from the skin friction of the flat plate. It is conventional to express the flat plate friction coefficient, C_{FP}, in terms of the surface area of the body. However, all coefficients in this paper other than C_{FP} are expressed in terms of the maximum frontal area of the body, A. Therefore, if C_F is the skin friction coefficient of the body, based on this frontal area, a relation is needed between C_{FP} and C_F.

The force due to skin friction on the body can be expressed as

$$F = C_{FP} S \rho v^2/2 \tag{11}$$

The force due to skin friction can also be expressed as

$$F = C_F A \rho v^2/2 \tag{12}$$

By combining Eqs. (11) and (12) we have the desired relation between C_F and C_{FP}.

$$C_F = (S/A)\, C_{FP} \tag{13}$$

By substituting Eq. (5) in Eq. (13)

$$C_F = 4(Q + \psi)\, C_{FP} \tag{14}$$

For turbulent flow along a flat plate, the skin friction coefficient can be determined from Schoenherr's equation.[3] For a limited range of Reynolds number, this equation is practically a straight line when plotted in a log-log graph and can be expressed as

$$C_{FP} = N(1/R_e)^n = N(\nu/Lv)^n \tag{15}$$

By combining Eqs. (14) and (15) we have

$$C_F = 4(Q+\psi) N (\nu/Lv)^n \tag{16}$$

TOTAL DRAG COEFFICIENT OF THE BODY

Applying Froude's method again, the total resistance of the body, or its corresponding coefficient, is equal to the sum of the frictional resistance and the residual resistance, or their corresponding coefficients

$$C_D = C_F + C_{DF} \tag{17}$$

RESIDUAL DRAG COEFFICIENT

Fig. 5 shows a typical installation in the High-Speed Water Tunnel of the model mounted on the three-component balances. (For description of balance system see Ref. 5). Models ranging from a slenderness ratio of 6.00 to 13.71 were mounted in a similar manner.

Fig. 7 shows the experimental results of determining the total drag coefficient versus Reynolds number for five different slenderness ratios of a body with nose and afterbody shape of the MK 13-1 torpedo (Fig. 6). From Eqs. (16) and (17) the residual drag coefficient versus Reynolds number can be calculated and plotted for each of the slenderness ratios on a log-log graph (Fig. 8).

Most of the resulting points fall very close to the straight line drawn through them in Fig. 8. The scatter represents approximately a plus or minus two percent variation of the *total* drag coefficient. Undoubtedly this scatter includes any variation due to the different slenderness ratios plus the accumulative error of the experimental measurements. Therefore any variation of the residual drag coefficient with a change in slenderness ratio must be much less than two per cent, so we are well justified in saying that the straight line of Fig. 6 represents the residual drag independent of the slenderness ratio. Thus, we can write

$$C_{DF} = M(1/R_e)^m = M(\nu/Lv)^m \tag{18}$$

and from Fig. 8, we can evaluate the coefficient M and the exponent m.

The results of determining the residual drag coefficients for other nose and afterbody shapes with fins is shown in the appendix. It will be noted that the same result is attained as shown in Fig. 8 for the MK 13-1 torpedo-shape nose and afterbody. Therefore, we conclude that for any one family of bodies of revolution the residual drag is a function of Reynolds number only as expressed in Eq. (18) and is independent of the slenderness ratio for all useful values. This relationship between C_{DF}, R_e, and L/D is shown in Fig. 9. Fig. 10 shows that this is true even for a blunt body down to a slenderness ratio of three. For any reasonably well shaped body the minimum slenderness ratio with no cylindrical midsection is great enough to insure the constancy of the residual drag.

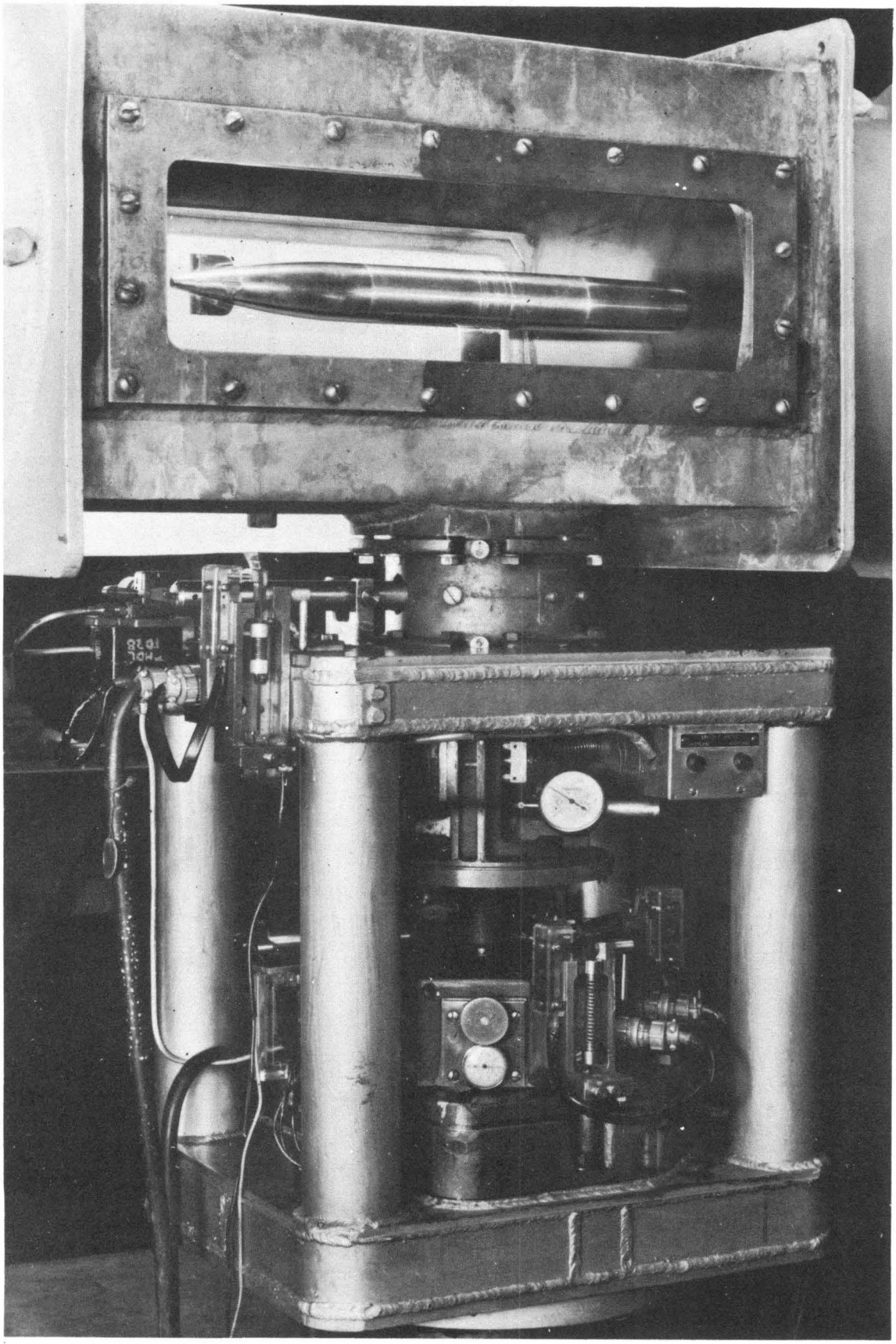

Fig. 5—Typical Installation For Determining Drag vs. Reynolds Number
Body is mounted on three-component balance. See Ref. 5.

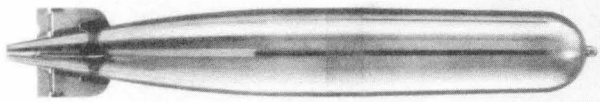

$(\psi) = 6.00$

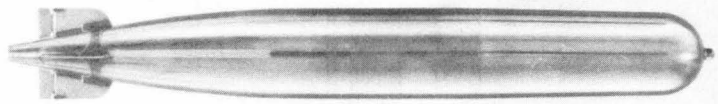

$(\psi) = 7.18$

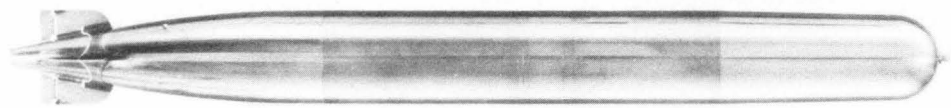

$(\psi) = 9.70$

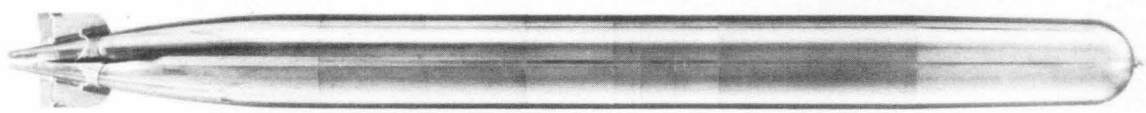

$(\psi) = 11.71$

$(\psi) = 13.71$

Fig. 6—Slenderness Ratio Study Series

In this series the nose and afterbody are the same as the MK 13-1 torpedo. These bodies were mounted in the High-Speed Water Tunnel at the California Institute of Technology, as shown in Fig. 5.

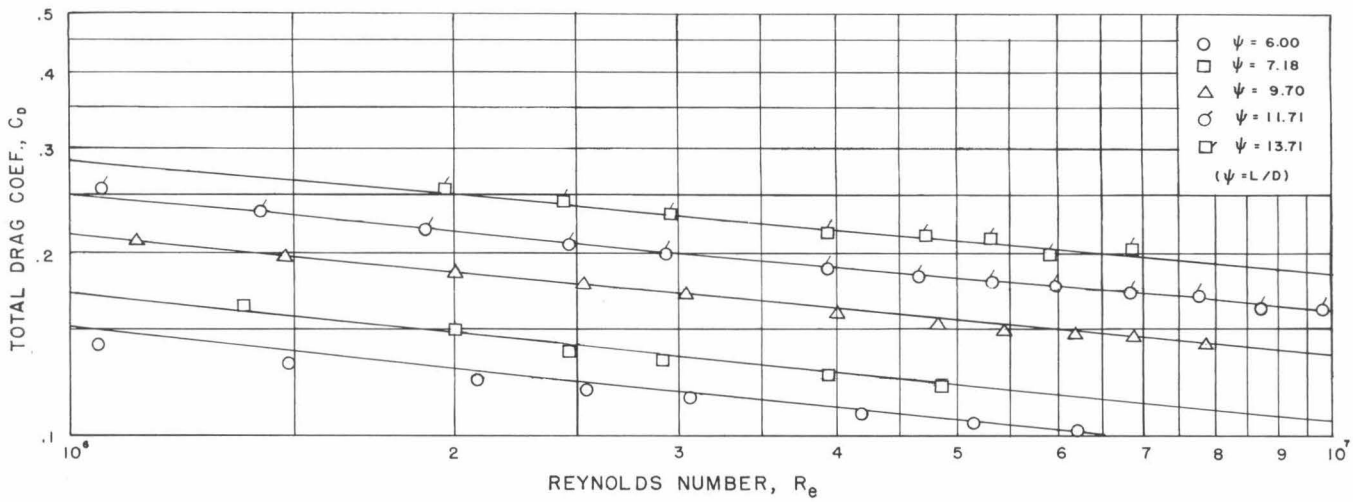

Fig. 7—Total Drag Coefficient vs. Reynolds Number

Reynolds number is based on the over-all length of the body. The experimental points were obtained using the two-inch diameter models shown in Fig. 6. The curves are plotted from Eq. (20).

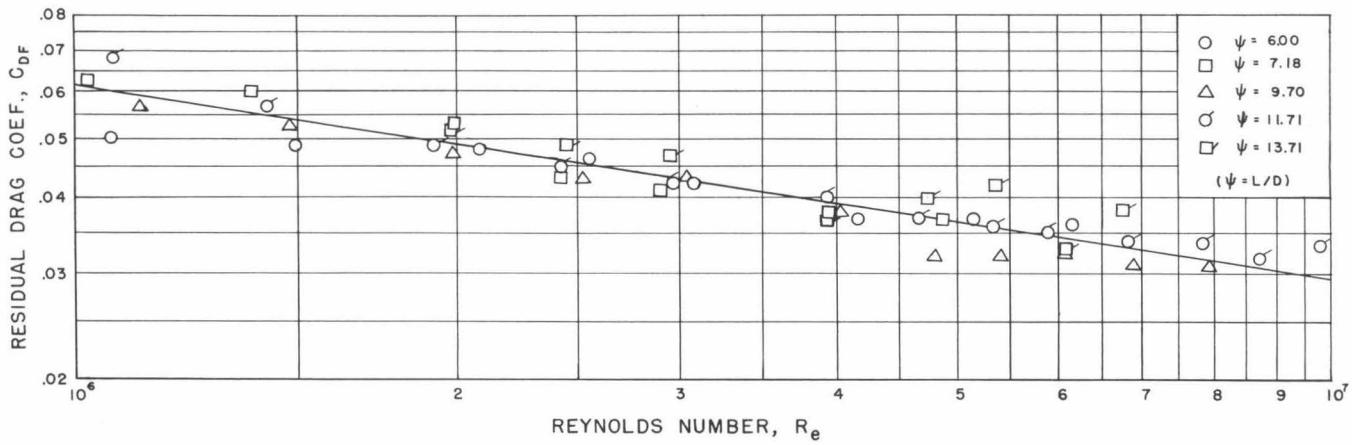

Fig. 8—Residual Drag Coefficient vs. Reynolds Number

The experimental points are calculated by using Eqs. (16) and (17).

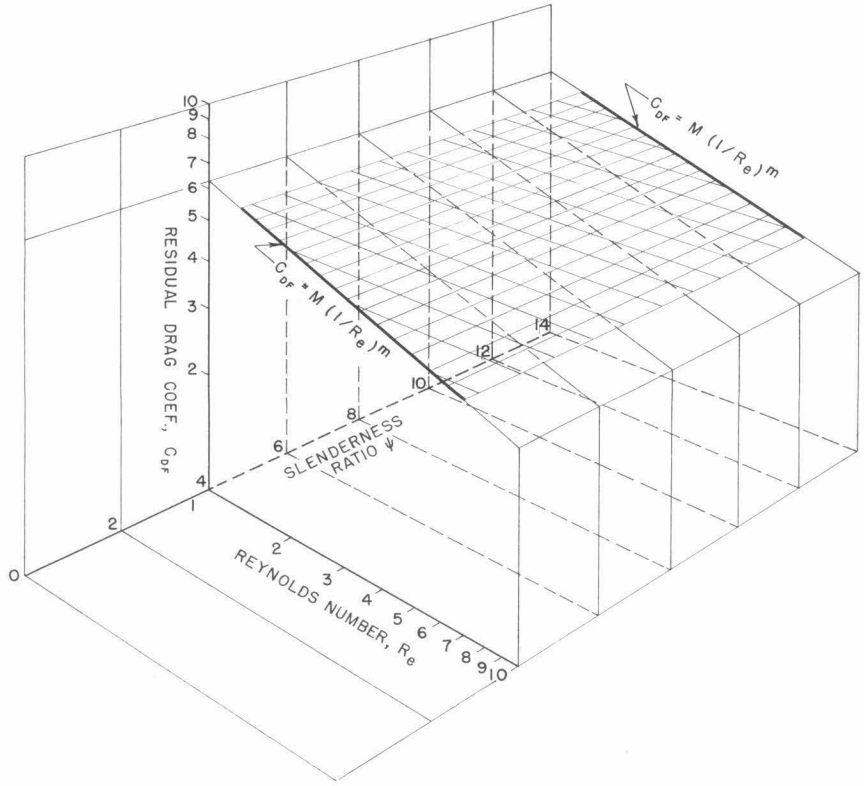

Fig. 9—Three-Dimensional Relation of C_{DF}, R_e, and L/D

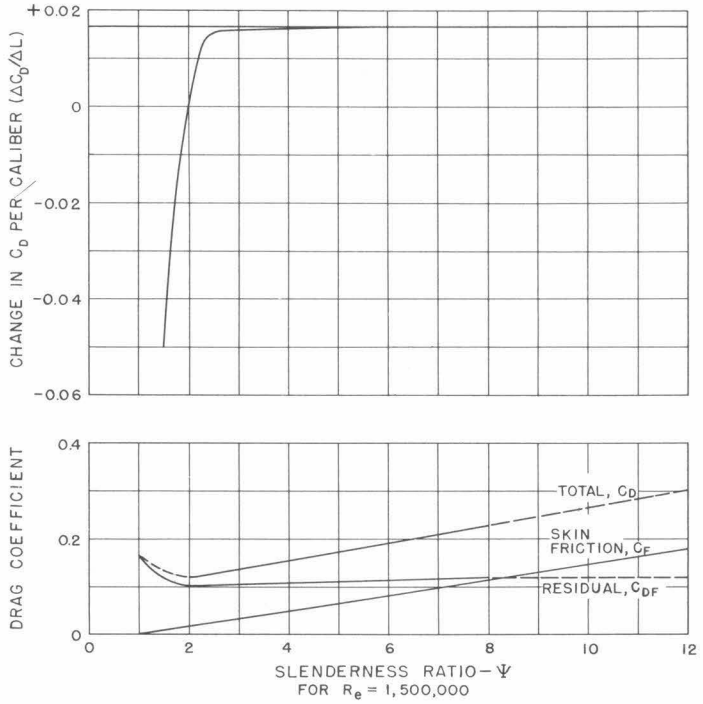

Fig. 10—Allocation of Residual Drag and Skin Friction for Cylinders with Hemispherical Ends

Col. Gerald B. Robison, at the time of his untimely death, left much valuable material in his unpublished work. The concept in Fig. 10, taken from his papers, suggested to the author the presentation given in this report.

TOTAL DRAG COEFFICIENT

It is now possible to express the total drag coefficient in terms of the slenderness ratio and the Reynolds number based on the volume of the body. This volume Reynolds number, R_v, is

$$R_v = vV^{1/3}/\nu \tag{19}$$

By substituting Eqs. (14, (15), and (18) in Eq. (17) we have

$$C_D = 4(Q+\psi)N(\nu/Lv)^n + M(\nu/Lv)^m \tag{20}$$

A check on the evaluation of Eq. (18) from Fig. 6 can now be made by calculating the total drag coefficient from Eq. (20). The curves in Fig. 7 are calculated from Eq. (20) and fit very closely to the experimental points.

By substituting Eqs. (10) and (19) in Eq. (20) we have

$$C_D = \frac{(Q+\psi)(B+\psi)^{n/3}}{R_v^n\ \psi^n}\ 4N(\pi/4)^{n/3} + \frac{(B+\psi)^{m/3}}{R_v^m\ \psi^m}\ M(\pi/4)^{m/3} \tag{21}$$

Another relation involving the total drag coefficient can be obtained by using the following relation with the drag force, F, acting on the body

$$F = C_D A\rho v^2/2 \tag{22}$$

or

$$F = C_D \pi D^2 \rho v^2/8 \tag{23}$$

Substitution of Eq. (9) in Eq. (23) gives the following convenient relation

$$C_D = \frac{F(B+\psi)^{2/3}}{v^2 V^{2/3}(\rho/2)(\pi/4)^{2/3}} \tag{24}$$

VELOCITY OF A BODY IN TERMS OF THE SLENDERNESS RATIO

By equating Eqs. (21) and (24) the total drag coefficient can be eliminated

$$\frac{1}{v^2 V^{2/3}} = \frac{1}{FR_v^n}\frac{(B+\psi)^{(n-2)/3}\ (Q+\psi)}{\psi^n} \times 4N(\rho/2)(\pi/4)^{(n+1)/3} + \frac{1}{FR_v^m}\frac{(B+\psi)^{(m-2)/3}}{\psi^m} \times M(\rho/2)(\pi/4)^{(m+1)/3} \tag{25}$$

Eq. (25) can be simplified by letting

$$E = \frac{(B+\psi)^{(n-2)/3}(Q+\psi)}{\psi^n} 4N(\rho/2)(\pi/4)^{(n+1)/3} \tag{26}$$

and

$$G = \frac{(B+\psi)^{(m-2)/3}}{\psi^m} M(\rho/2)(\pi/4)^{(m+1)/3} \tag{27}$$

After substituting Eqs. (26) and (27) in Eq. (25), and multiplying through by R_v^n (remembering that $R_v^n = v^n V^{n/3}/\nu^n$), Eq. (25) reduces to

$$v = \frac{F^{1/(2-n)}\ V^{(n-2)/3(2-n)}}{[\nu^n(E+GR_v^{(n-m)})]^{1/(2-n)}} \tag{28}$$

FREE SINKING BODY

Let us assume that the body is sinking vertically in water and has reached its terminal velocity. The force acting on the body due to gravity is

$$F = \Delta\gamma V \tag{29}$$

where $\Delta\gamma$ is the negative buoyancy of the body in water, lbs. per ft^3. Substituting Eq. (29) in Eq. (28) gives the terminal velocity of a free sinking body

$$v = \frac{\Delta\gamma^{1/(2-n)}\ V^{(n+1)/3(2-n)}}{[\nu^n(E+GR_v^{(n-m)})]^{1/(2-n)}} \tag{30}$$

The effect of changing the slenderness ratio on the sinking rate can be seen by using a graphical solution of Eq. (30). The denominator is plotted as the "characteristic curve" in Fig. 11 for an average value of R_v based on the range of volumes and velocities indicated in the same Fig. 11. For the range of volumes

and negative buoyancies indicated on the chart, the characteristic curve based on an average value of R_v gives a close approximation to the free sinking velocity. Fig. 11 is based on the MK 13-1 torpedo shape. The volume and negative buoyancy range in these three charts were selected to approach that of a depth charge.

The following method is used to determine the velocity of a free sinking body with the MK 13-1 nose and afterbody shape. Assume the slenderness ratio of the body is 6.5, the volume of the body is 5 ft^3, and the negative buoyancy is 50 lbs. per ft^3. Turn to Fig. 11 and select the slenderness ratio. Move vertically to the characteristic curve, horizontally to the volume of the body, vertically to the negative buoyancy, then horizontally to the terminal velocity scale, reading 59 ft. per sec.

As mentioned before, the characteristic curve in Fig. 11 is calculated for an assumed average value of R_v. This value appears in the denominator of Eq. (30), therefore if the value of R_v changes, there is a change in the terminal velocity. Fig. 12 is a chart similar to Fig. 11, but it has been constructed to allow for this variation of R_v. A change in R_v effects directly the characteristic curve, therefore in Fig. 12 three curves have been drawn which cover the range of volumes and velocities shown on the chart. A trial and error solution is now necessary. Select the slenderness ratio and the the volume, and assume a value for R_v; use the chart in the same manner as indicated for Fig. 11 and obtain a terminal velocity. Use this terminal velocity to calculate a new value for R_v. Repeat the above process until the calculated value of R_v is the same as the assumed value.

HORIZONTALLY MOVING BODY

A chart similar to Fig. 11 can be made for a body moving in a horizontal plane without acceleration. Let us assume that the input horsepower, P_H, and the over-all efficiency, η, are known. If P is the theoretical horsepower, we can write

$$P = Fv \tag{31}$$

and

$$P = P_H \eta 550 \tag{32}$$

or

$$F = P_H \eta 550/v \tag{33}$$

Substitute Eq. (33) in Eq. (28) and we have the velocity of a horizontally moving body in terms of its slenderness ratio, volume, input horsepower, over-all efficiency, and R_v.

$$v = \frac{(P_H \eta 550)^{1/(3-n)} V^{(n-2)/3(3-n)}}{[\nu^n (E + G R_v^{(n-m)})]^{1/(3-n)}} \tag{34}$$

As in the case of the free sinking body, Fig. 13 shows the effect of changing the slenderness ratio. The denominator is also plotted as the "characteristic curve" for an average value of R_v based on the range of volumes and velocities indicated in Fig. 13.

CONSTANT RESIDUAL DRAG FOR A FREE SINKING BODY

If the flow pattern over the body does not vary with a changing Reynolds number, then the residual drag of the body will be constant and m in Eq. (18) will be zero. Therefore M equals C_{DF} and Eq. (27) becomes

$$G' = \frac{C_{DF}(\rho/2)(\pi/4)^{1/3}}{(B+\psi)^{2/3}} \tag{35}$$

and Eq. (30) becomes

$$v = \frac{\Delta \gamma^{1/(2-n)} V^{(n+1)/3(2-n)}}{[\nu^n (E + G' R_v^n)]^{1/(2-n)}} \tag{36}$$

Fig. 14 is an example of Eq. (36) and is calculated for an assumed form drag value of 0.013 and the same average value of R_v as used in Fig. 11. If the two charts are compared, it will be noted that the terminal velocities are approximately the same for a given slenderness ratio, volume of body and negative buoyancy.

CONSTANT RESIDUAL DRAG FOR A HORIZONTALLY MOVING BODY

As mentioned for a free sinking body, m equals zero and M equals C_{DF} when the residual drag is constant with Reynolds number. Therefore, Eq. (34) becomes

$$v = \frac{(P_H \eta 550)^{1/(3-n)} V^{(n-2)/3(3-n)}}{[\nu^n (E + G' R_v^n)]^{1/(3-n)}} \tag{37}$$

The residual drag coefficient of a body the size of a submarine is probably constant. If the submarine is a "clean" shape, we believe that a conservative estimate of this coefficient would be 0.02.

It is shown later in this paper that for normally shaped bodies the surface area and volume shape parameters have little effect on the optimum slenderness ratio.

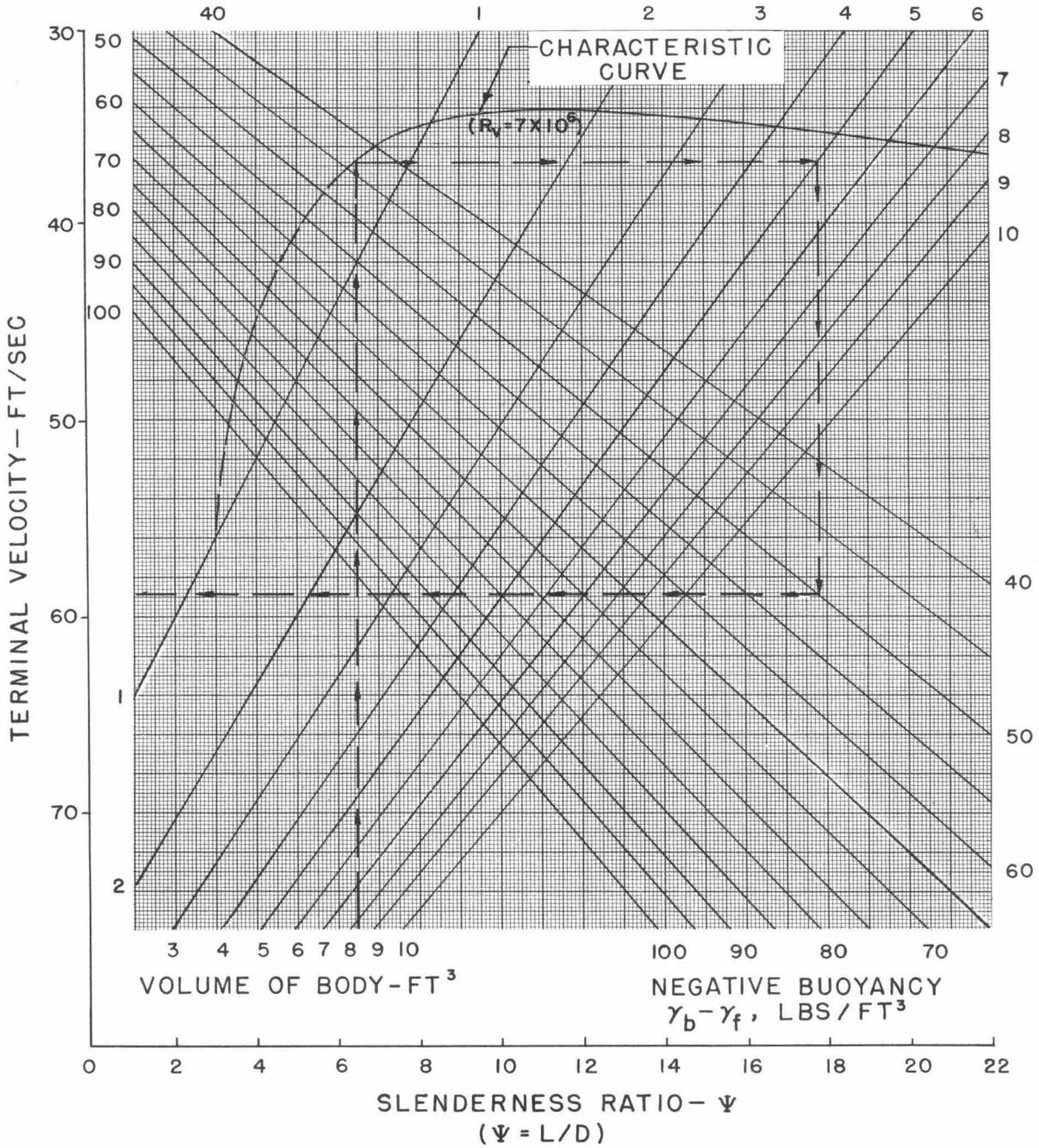

Fig. 11—Sinking Body Velocity Chart for MK 13-1 Torpedo Nose and Afterbody Shape for Average Value of Volume Reynolds Number

This chart is designed for a free sinking body of a size and velocity range suitable for a depth charge. The characteristic curve is calculated on the basis of the data in Fig. 8, and for an average volume Reynolds number based on the range of velocities and volumes indicated in the chart.

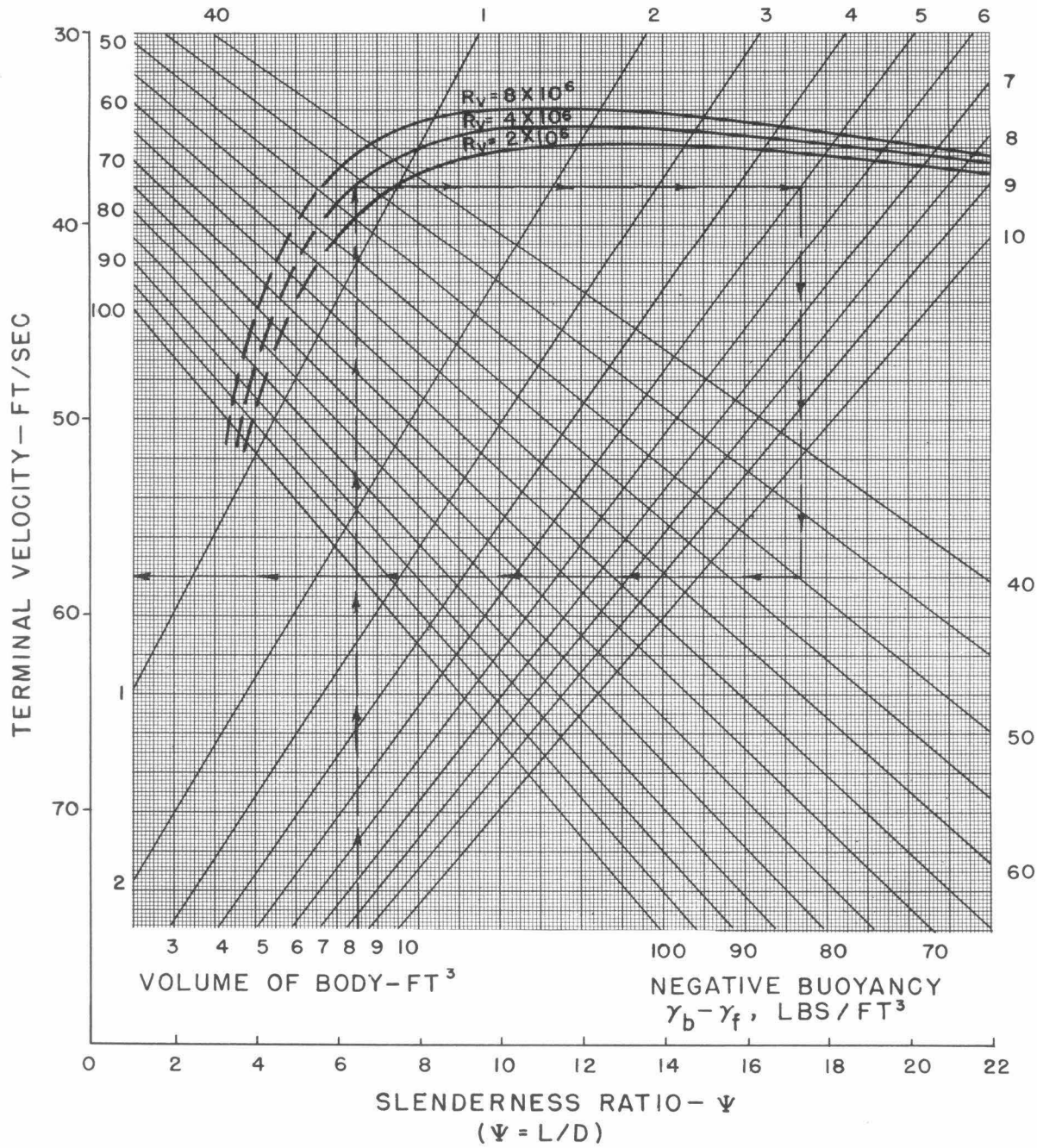

Fig. 12—Sinking Body Velocity Chart for MK 13-1 Torpedo Nose and Afterbody Shape for Several Values of the Volume Reynolds Number.

The characteristic curves are calculated for several values of R_v which cover largely the range of velocities and volumes indicated on the chart. This chart is otherwise the same as Fig. 11.

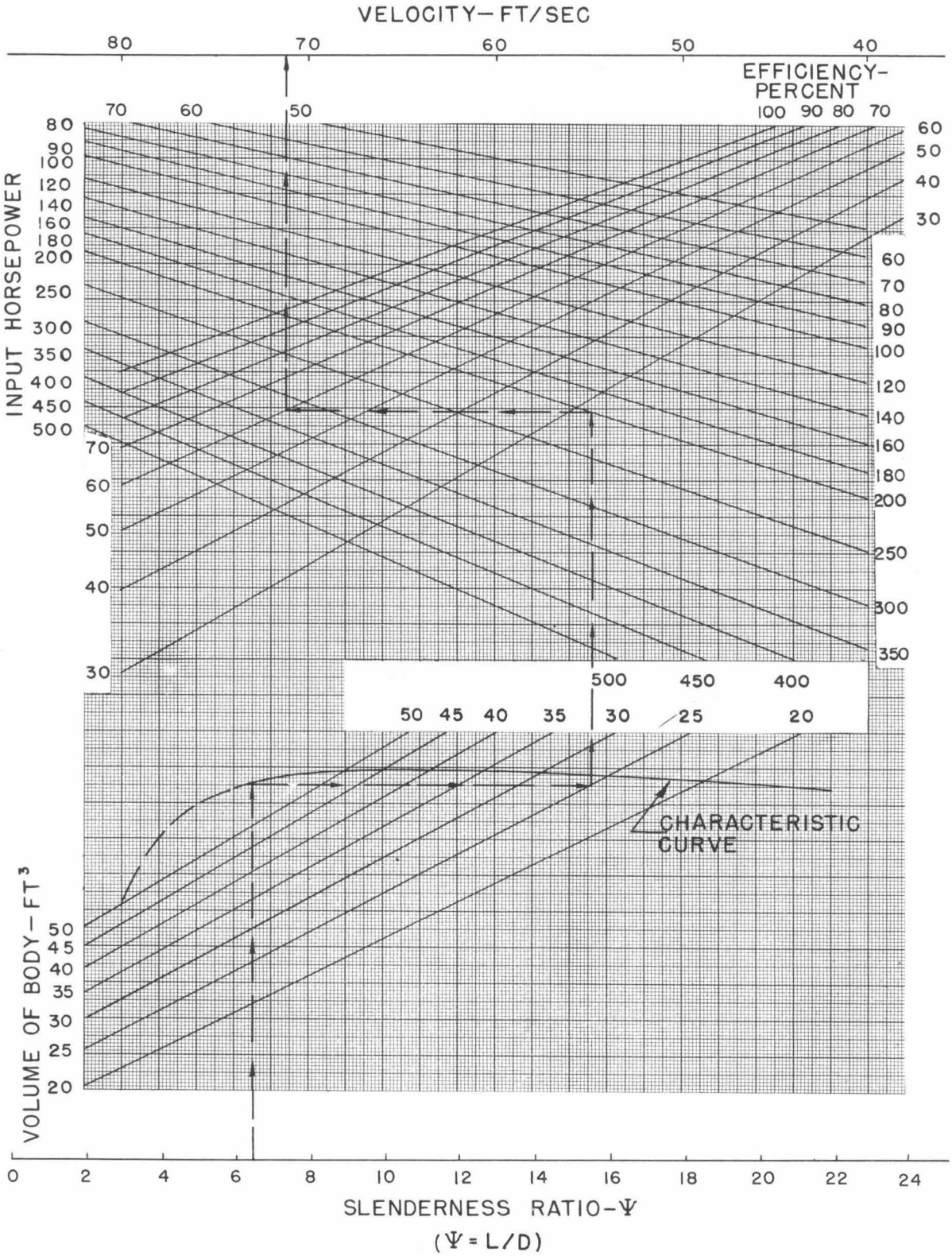

Fig. 13—Horizontally Moving Body Velocity Chart for MK 13-1 Torpedo Nose and Afterbody Shape for Average Value of Volume Reynolds Number

This chart is designed for a horizontally moving body in the size and horsepower range of the torpedo. The characteristic curve is calculated on the same basis as the characteristic curve in Fig. 11.

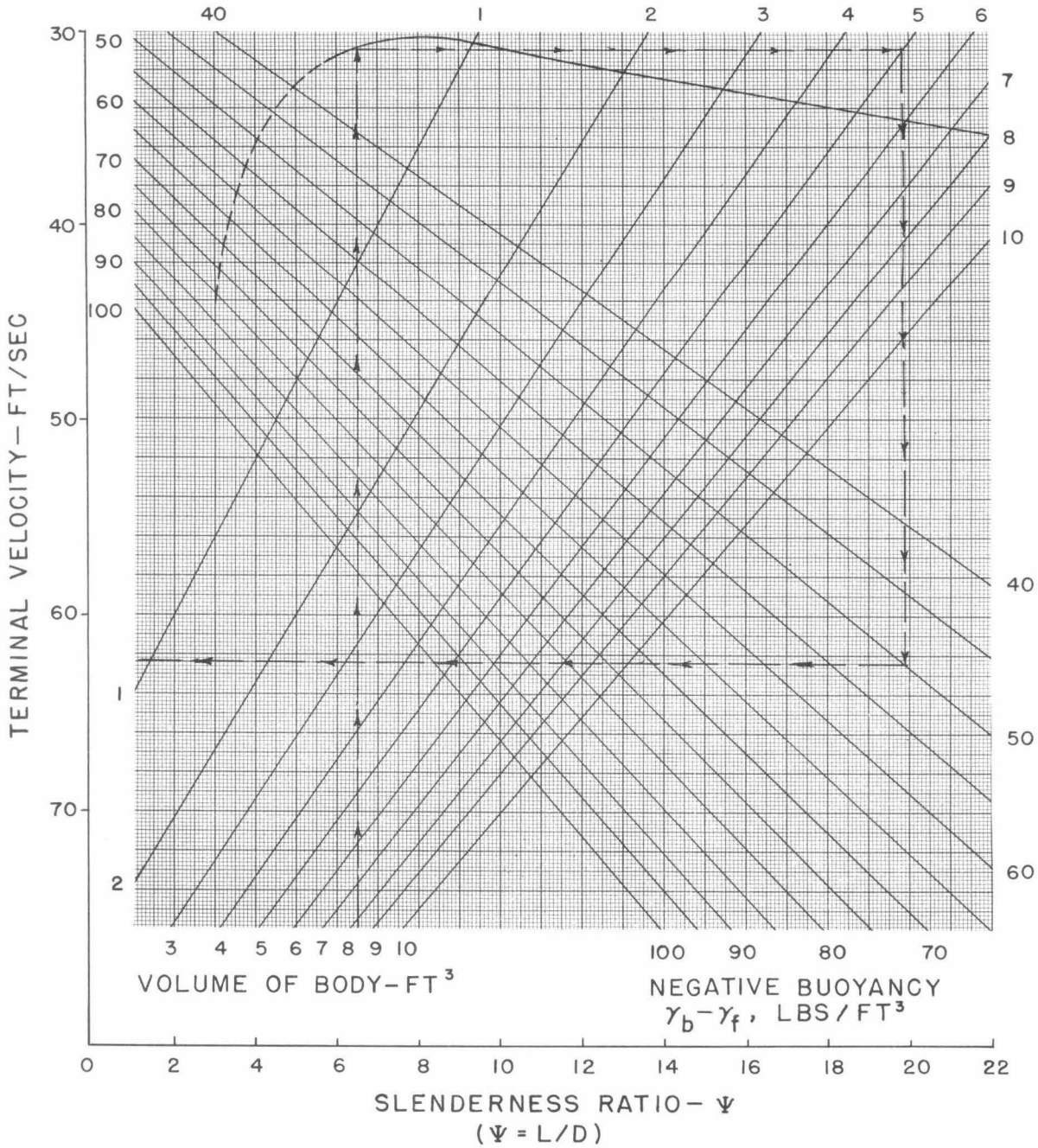

Fig. 14—Sinking Body Velocity Chart for MK 13-1 Torpedo Nose and Afterbody Shape for Constant Residual Drag Coefficient

The characteristic curve is calculated for an assumed constant residual drag value of 0.013 and the same average value of R_v used in Fig. 11.

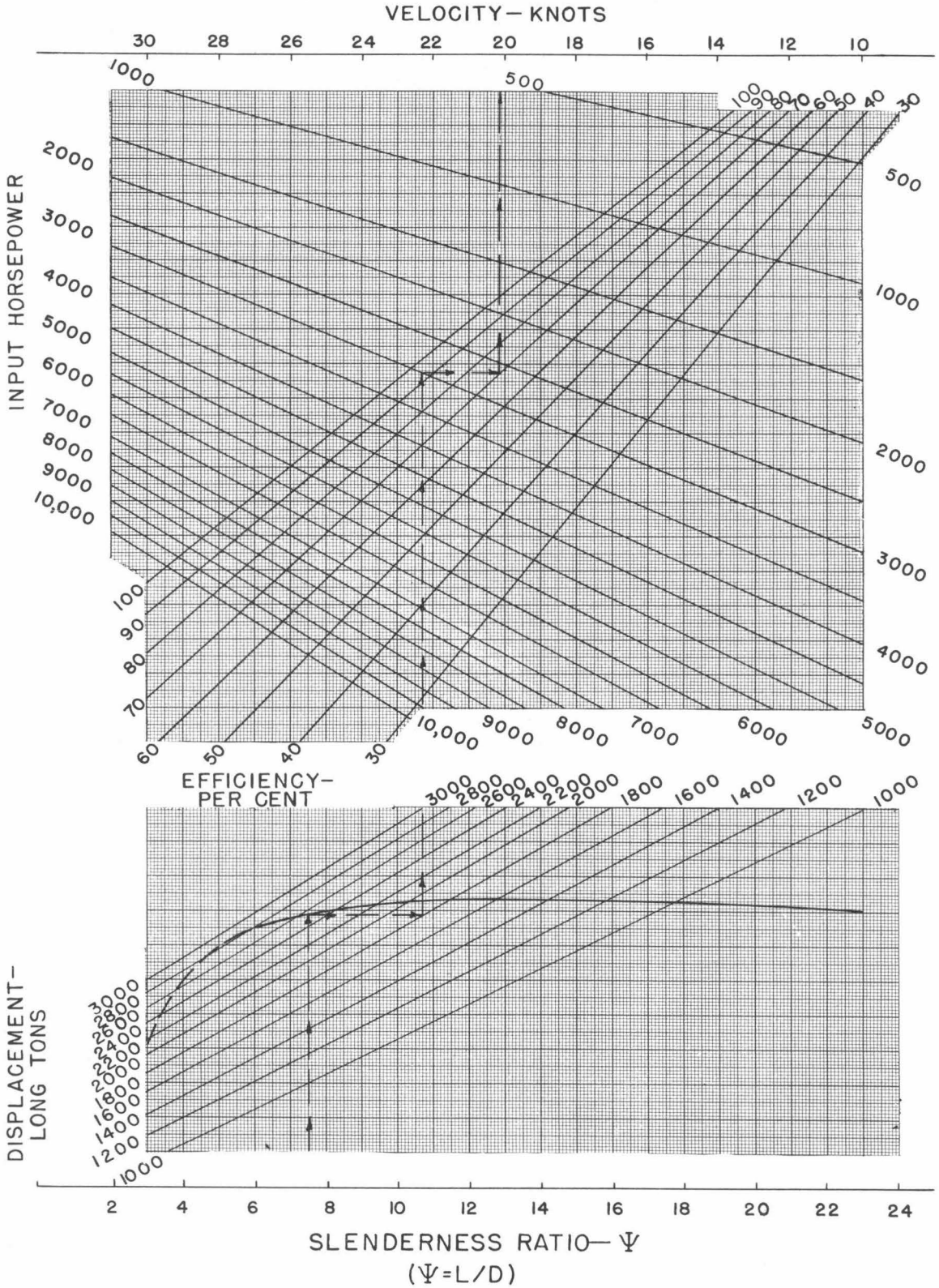

Fig. 15—Velocity Chart for a Hypothetical Submarine

The characteristic curve is calculated for a $R_v = 10^8$ and constant residual drag coefficient equal to 0.02.

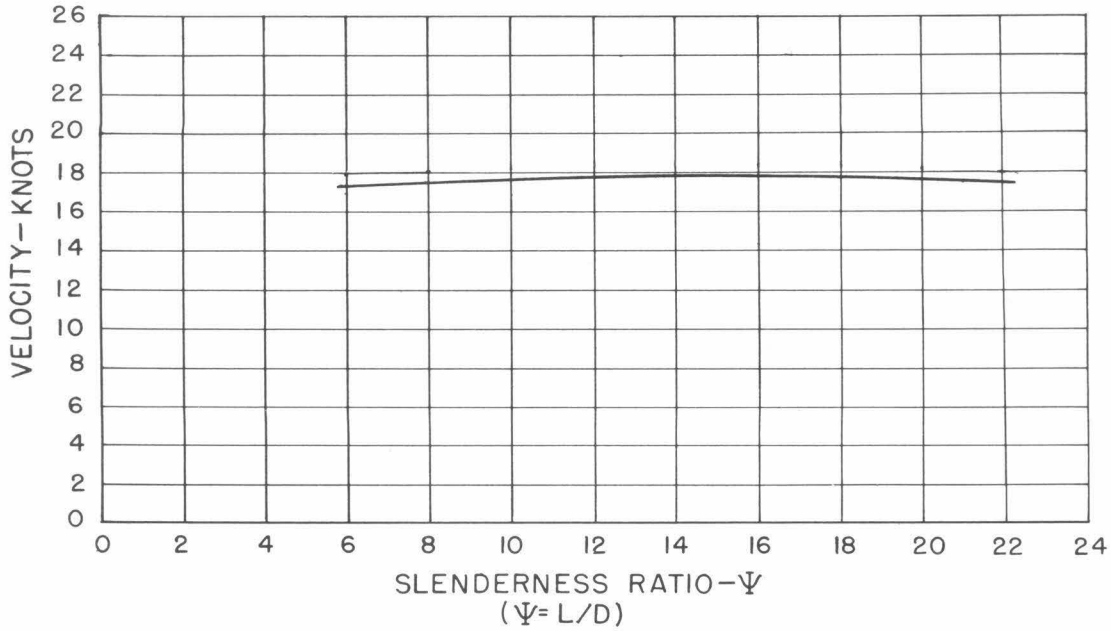

Fig. 16—Relation of Slenderness Ratio to Velocity for a Submarine of Given Displacement and Horsepower

Curve is calculated for the same hypothetical shape as in Fig. 15 and for a displacement of 2,000 long tons, 2,500 input horsepower and 60 per cent over-all efficiency.

Therefore, Fig. 15 has been calculated as an example of Eq. (37) for an assumed constant residual drag coefficient of 0.02 and for the shape of the MK 13-1 torpedo whose shape parameters roughly approximate those of a submarine.

Fig. 16 is an example of Eq. (37) in which the volume of the body, the horsepower, and the efficiency have been assumed to have a constant value. We, therefore, have a picture of the direct effect of changing the slenderness ratio. As can be seen from Fig. 16, a rather large change in the slenderness ratio has a small effect on the velocity of the body.

CONSTANT TOTAL DRAG FOR A FREE SINKING BODY

If the body is sufficiently rough, the total drag coefficient may be constant for large values of Reynolds number. Here the residual drag and the frictional drag coefficients are constant with Reynolds number. As previously mentioned, if the residual drag is constant with Reynolds number, m equals zero and M equals C_{DF}. It follows in like manner that if the skin friction does not vary with Reynolds number, n in Eq. (15) will be zero and N will equal C_{FP}. For these conditions Eq. (26) becomes

$$E' = \frac{(Q+\psi)}{(B+\psi)^{2/3}} \, 4\, C_{FP} \, (\rho/2)(\pi/4)^{1/3} \tag{38}$$

and Eq. (30) becomes

$$v = \frac{\Delta \gamma^{1/2} V^{1/6}}{(E'+G')^{1/2}} \tag{39}$$

Fig. 17 is an example of Eq. (39). Note that R_v does not enter into Eq. (39) and, therefore, the characteristic curve shown on Fig. 17 is unique for the particular shape (MK 13-1 or MK 14-1) for which it was calculated.

CONSTANT TOTAL DRAG COEFFICIENT FOR HORIZONTALLY MOVING BODY

As mentioned for the free sinking body, n and m equal zero, M equals C_{DF}, and N equals C_{FP} for a horizontally moving body when the total drag coefficient is constant with Reynolds number. Therefore Eq. (34) becomes

$$v = \frac{(P_H \eta 550)^{1/3} V^{-2/9}}{(E'+G')^{1/3}} \tag{40}$$

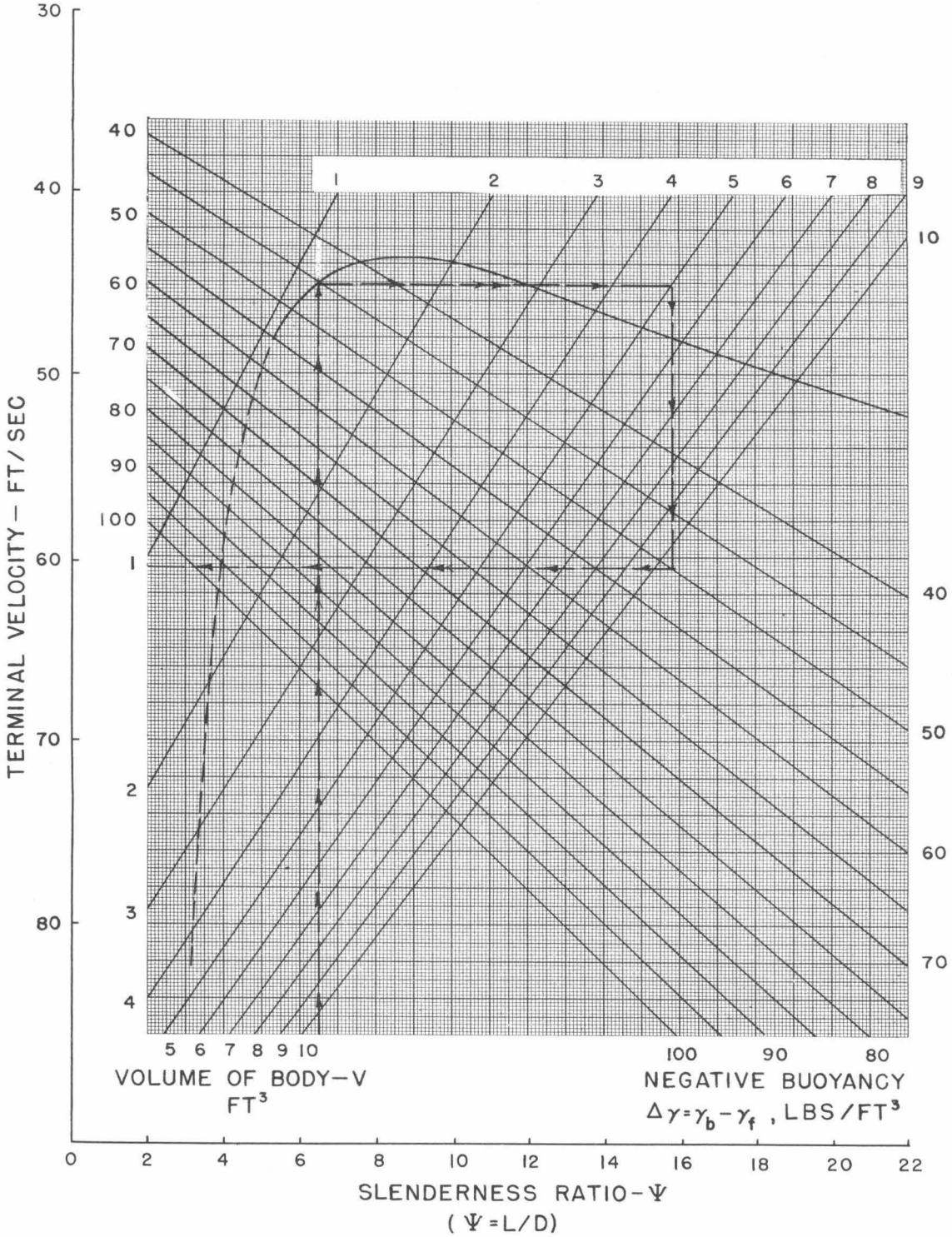

Fig. 17—Sinking Body Velocity Chart for MK 13-1 Torpedo and Afterbody Shape for Constant Total Drag Coefficient.

The characteristic curve is calculated for an assumed constant residual drag value of 0.013 and an assumed constant skin friction value of 0.00229.

MAXIMUM POINT OF THE CHARACTERISTIC CURVE

It will be noted that the maximum velocity is attained for a slenderness ratio which passes through the peak of the characteristic curve. The location of the maximum of this curve indicates for a particular body the optimum slenderness ratio. This can be determined with sufficient accuracy for most uses by visual inspection of the characteristic curve, due to the fact that the curve is fairly flat in the immediate vicinity of the maximum.

The tedious work involved in the differentiation of the equation of the characteristic curve therefore is not justified merely to find the maximum point. However, by differentiating and setting the resulting equation equal to zero, we can observe why different bodies will have different optimum points. We will then be in a position to compare directly several different shapes and to show the effect of varying the residual drag, the volume Reynolds number and the surface area of the body.

Examination of either Eq. (30) or Eq. (34) shows that the determination of the minimum of the following relation will give the maximum of the characteristic curve for either a free sinking body or a horizontally moving body.

$$F(\psi) = E + GR_v^{(n-m)} \tag{41}$$

Let

$$K_1 = 4N(\rho/2)(\pi/4)^{(n+1)/3} \tag{42}$$

and

$$K_2 = M(\rho/2)(\pi/4)^{(m+1)/3} \tag{43}$$

then Eq. (41) can be written

$$F(\psi) = \frac{\psi^m(B+\psi)^{(n-2)/3}(Q+\psi)K_1 + \psi^n(B+\psi)^{(m-2)/3}}{\psi^{(n+m)}} \tag{44}$$

In order to find the minimum point of Eq. (44) we must differentiate it, set it equal to zero, multiply through by

$$\frac{3}{\psi^{(n+2m-1)}(B+\psi)^{(n-5)/3}(1-2n)}$$

and combine terms and we have

$$F'(\psi) = 0 = \psi^2 + \frac{[3B(1-n)-2Q(1+n)]}{(1-2n)}\psi - \frac{BQ}{(1-2n)} + \frac{R_v^{(n-m)}M}{4N(\pi/4)^{(n-m)/3}(1-2n)} \times \left[\frac{(m-2)\psi^{(n-m+1)}}{(B+\psi)^{(n-m)/3}} - \frac{3m\psi^{(n-m)}}{(B+\psi)^{(n-m-3)/3}}\right] \tag{45}$$

Let

$$F_1(\psi) = \psi^2 + \frac{[3B(1-n)-2Q(1+n)]}{(1-2n)}\psi - \frac{BQ}{(1-2n)} \tag{46}$$

and let

$$F_2(\psi) = \frac{R_v^{(n-m)}M}{4N(\pi/4)^{(n-m)/3}(1-2n)} \times \left[\frac{(m-2)\psi^{(n-m+1)}}{(B+\psi)^{(n-m)/3}} - \frac{3m\psi^{(n-m)}}{(B+\psi)^{(n-m-3)/3}}\right] \tag{47}$$

or

$$F'(\psi) = 0 = F_1(\psi) + F_2(\psi) \tag{48}$$

$F_1(\psi)$ is a dimensionless function which involves only surface area, volume and slenderness ratio, and is unaffected by the excellence of the body shape.

$F_2(\psi)$ is also dimensionless and is a function of the slenderness ratio, residual drag and Reynolds number, R_v, and may be considered as a scale of residual drag.

By plotting $F_1(\psi)$ and the negative of $F_2(\psi)$ as shown in Fig. 18, the intersection of these two curves will give the maximum point (*i.e.*, the solution of Eq. (48)). Fig. 18 is plotted for the same values of the coefficients as Fig. 11 and, therefore, the slenderness value as determined by the intersection fixes the maximum point of the characteristic curve in Figs. 11 and 13. Thus, we see that the optimum slenderness ratio for the MK 13-1 torpedo shape when R_v equals 7×10^6 is 11.5. Fig. 21 likewise gives the maximum point of Figs. 31 and 32 for the MK 14-1 torpedo shape.

By using the method just described to determine the maximum point of the characteristic curve, it is possible to obtain a clear picture of the effect of the various parameters on the optimum slenderness ratio. The parameters involved in the determination are:

- B, a constant for a given shape and dependent on the volume of the nose and afterbody (see Eq. (7)).
- Q, a constant for a given shape and dependent on the surface area of the nose and afterbody (see Eq. (4)).
- N, coefficient in the skin friction relation for a flat plate (see Eq. (15)) and assumed to be independent of the shape of the body.

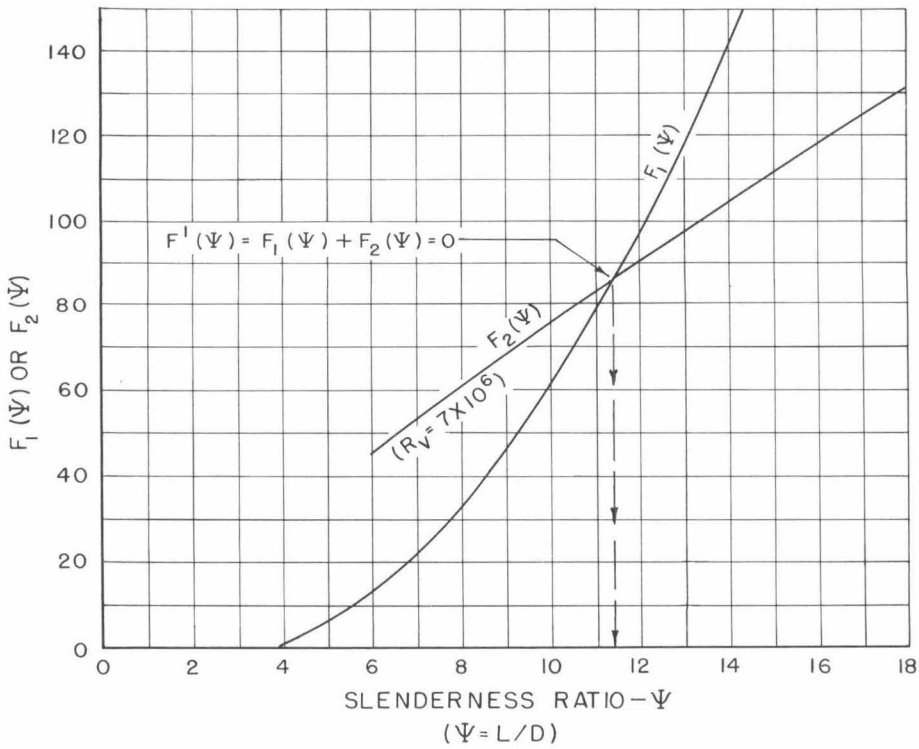

Fig. 18—Maximum Point Chart for MK 13-1 Torpedo Nose and Afterbody Shape
The intersection of the two curves gives the maximum point of the characteristic curve in Figs. 11 and 13.

n, exponent in the skin friction relation for a flat plate (see Eq. (15)) and assumed to be independent of the shape of the body. For the case of a rough body, n is assumed to be zero.

M, coefficient in the residual drag relation (see Eq. (18)) constant for a given nose and afterbody shape as indicated in Fig. 8.

m, exponent in the residual drag relation (see Eq. (18)) and constant for a given nose and afterbody shape as indicated in Fig. 8. If it is assumed that the body has constant residual drag, then m equals zero. For the case of a rough body, it is assumed that m equals zero.

R_v, Reynolds number based on the volume of the body (see Eq. (19)).

EFFECT OF THE RESIDUAL DRAG

In order to determine the effect of different values of the residual drag on the slenderness ratio, it is convenient to assume that for a given body the residual drag remains constant with Reynolds number, R_e.

The above assumption means that m equals zero and, therefore, M equals C_{DF}. There will be no change in (46) but Eq. (47) becomes

$$F_2(\psi) = -\frac{R_v^n C_{DF} \psi^{(n+1)}}{4N(\pi/4)^{n/3}(1-2n)(B+\psi)^{n/3}} \qquad (49)$$

Using the MK 14-1 nose and afterbody shape as an example, $F_1(\psi)$ in Fig. 20 is the same as in Fig. 19. $F_2(\psi)$ is calculated from Eq. (49) for various values of C_{DF}. We can immediately see that the optimum slenderness ratio of a body is very dependent on its residual drag. Thus for this particular body, the minimum slenderness ratio is approximately 7, whereas a residual drag of 0.030 (which is possible with a poor nose) indicates an optimum ratio greater than 15.

SOME TYPICAL BODY SHAPES

Fig. 21 shows some body shapes which are considered in this paper. In order to compare their comparative shapes more easily, the bodies have been superimposed on each other. Eq. (46) has been evaluated for several of these bodies and plotted in Fig. 22.

Examination of Eq. (49) shows that this equation changes very little for various body shapes because the term involving the volume parameter B is raised to a small power. Therefore, in Fig. 22, the various $F_2(\psi)$ curves are the same as those used in Fig. 20.

We can conclude from this chart that certain bodies, with all other factors the same, will have lower optimum slenderness ratios than others. We can *not* tell from this chart which shape is the "best." The Lyon Form "A"[4] is without fins and therefore unstable.

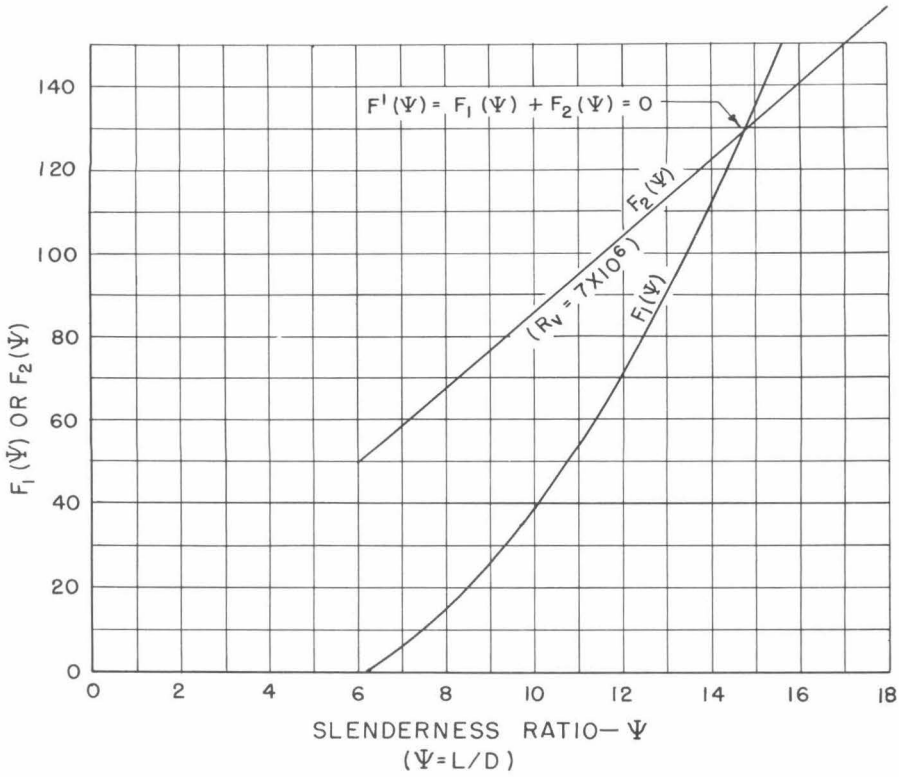

Fig. 19—Maximum Point Chart for MK 14-1 Torpedo Nose and Afterbody Shape

The intersection of the two curves gives the maximum point of the characteristic curve in Figs. 31 and 32.

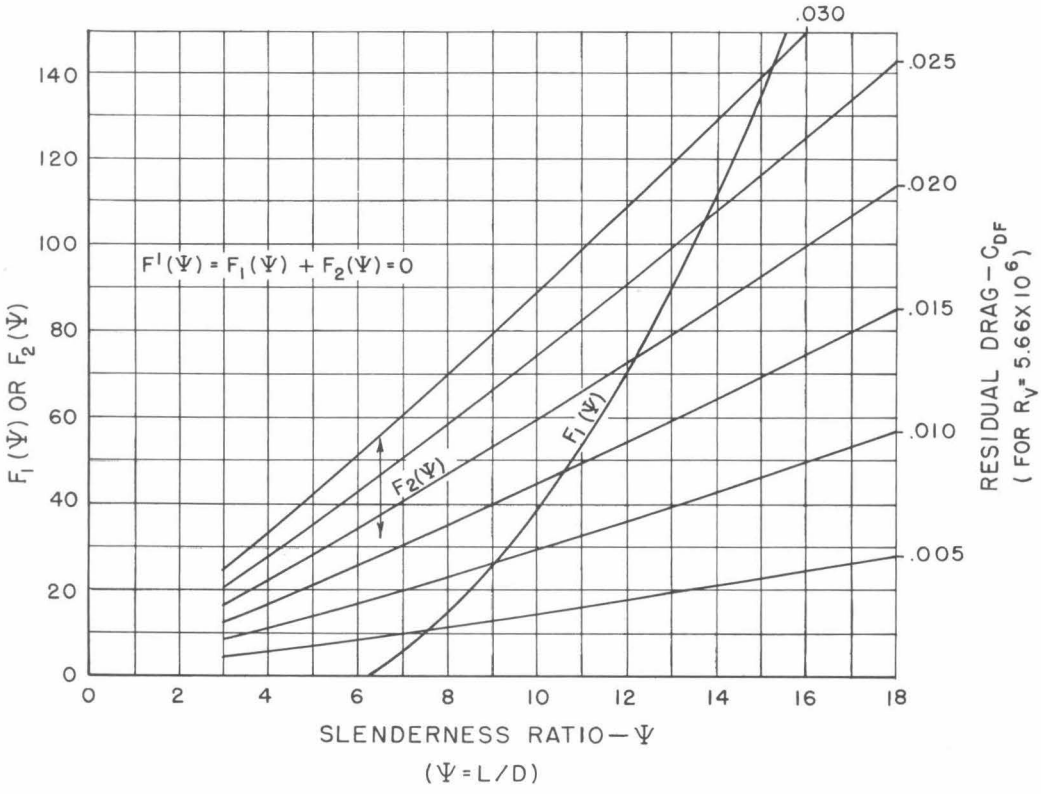

Fig. 20—Effect of the Residual Drag

The $F_1(\psi)$ curve is calculated for the MK 14-1 torpedo nose and afterbody shape.

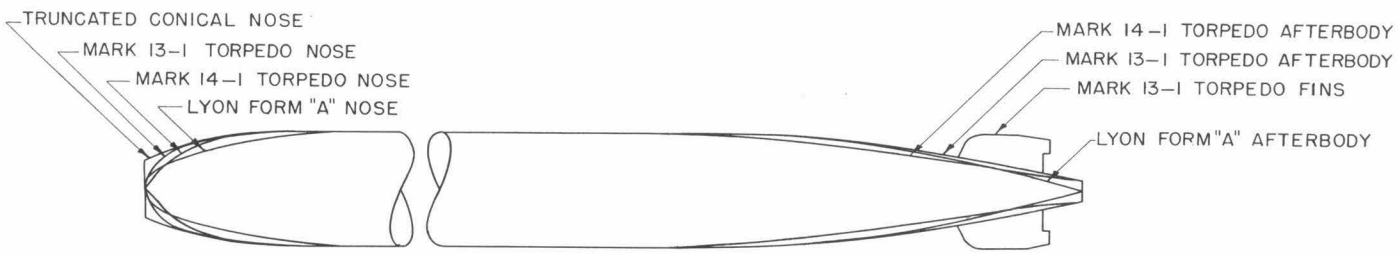

Fig. 21—Comparison of Nose and Afterbody Shapes

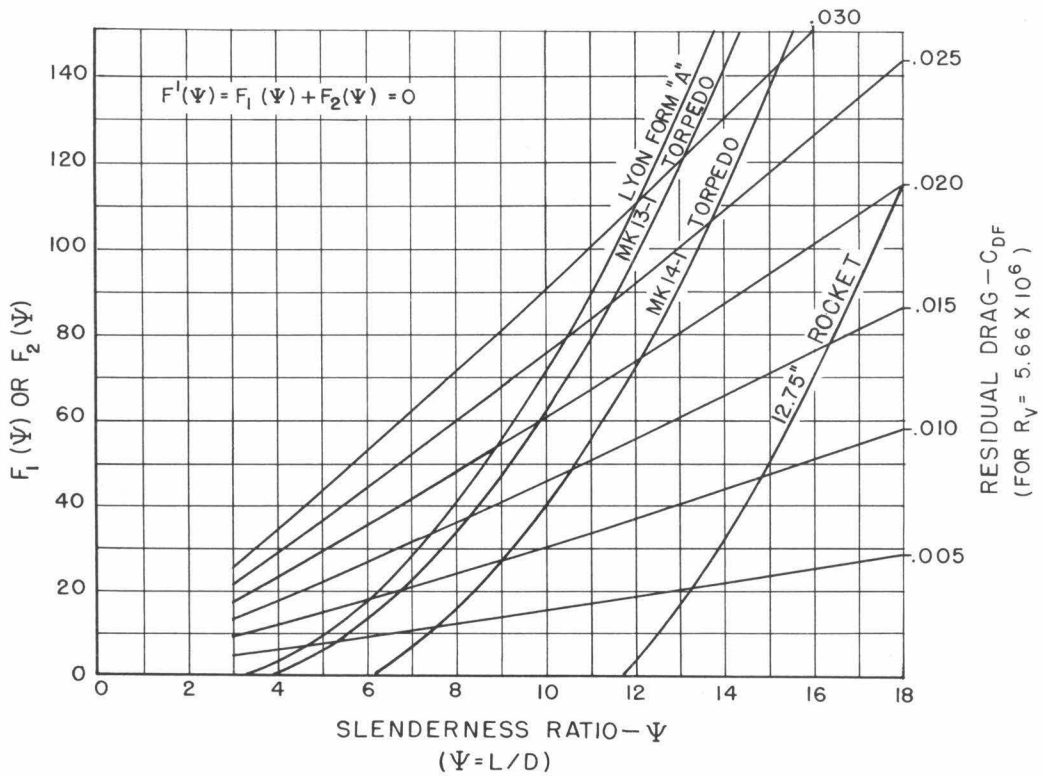

Fig. 22—Effect of Several Body Shapes on the Maximum Point

EFFECT OF INCREASING THE SURFACE AREA OF A BODY

As the Lyon Form "A" has a low residual drag, it is a desirable shape for the nose and afterbody sections of an underwater body. Therefore, attention is given here to the effect of increasing its surface area, either by adding cylindrical midsections or by adding stabilizing fins. Fig. 23 is an outline of the Lyon Form "A" with imaginary fins drawn in. To have a convenient means of expressing the surface area percentagewise, independent of a change in slenderness ratio, imagine that the body is enclosed by a cylinder the same length as the body.

In Fig. 24 the various $F_2(\psi)$ curves are again the same as those used in Fig. 22. The $F_1(\psi)$ curves in Fig. 24 are plotted for a range of 80 to 110 per cent of the surface area of the enclosing cylinder (ends not included). The limiting curve on the left is for the bare body without fins. The addition of fins to the bare body will cause an appreciable increase in the surface area. For this body to be stable, we conclude that the optimum slenderness ratio will probably be greater than the minimum possible value of five.

Fig. 23—Lyon Form "A" Body Enclosed by a Cylinder

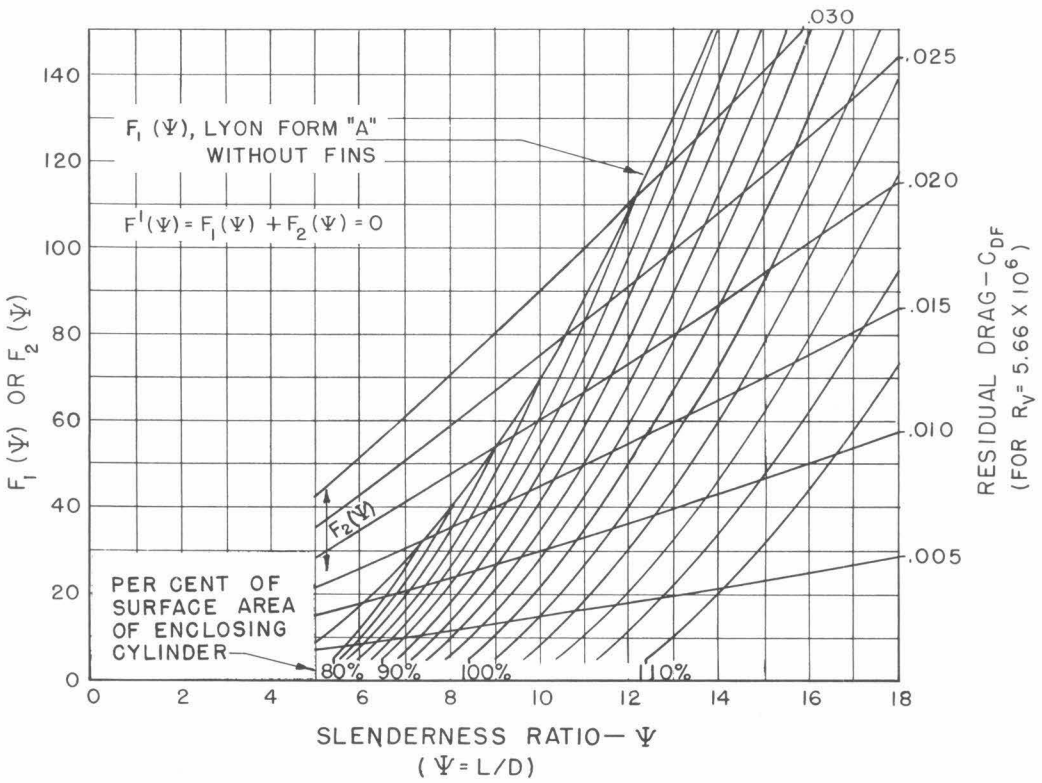

Fig. 24—Effect of Varying the Surface Area of a Body

It is assumed that there is no change in the body shape and that the area is increased by the addition of fins, etc.

EFFECT OF CHANGING THE VOLUME REYNOLDS NUMBER

If the slope of the residual drag curve is the same as that of the flat plate curve ($m=n$) then

$$R_v^{(n-m)} = 1$$

and the volume Reynolds number has no effect on the optimum value of the slenderness ratio. However, if the slope of the residual drag curve is greater than that of the flat plate ($m>n$), an increase in the value of R_v decreases the optimum slenderness ratio (see Fig. 25). On the other hand, if the slope of the residual drag curve is less than that of the flat plate or equal to zero, an increase in R_v causes an increase in the optimum slenderness ratio (see Fig. 26).

It is therefore impossible to make a general statement as to the effect of changing volume Reynolds number on the optimum value of the slenderness ratio.

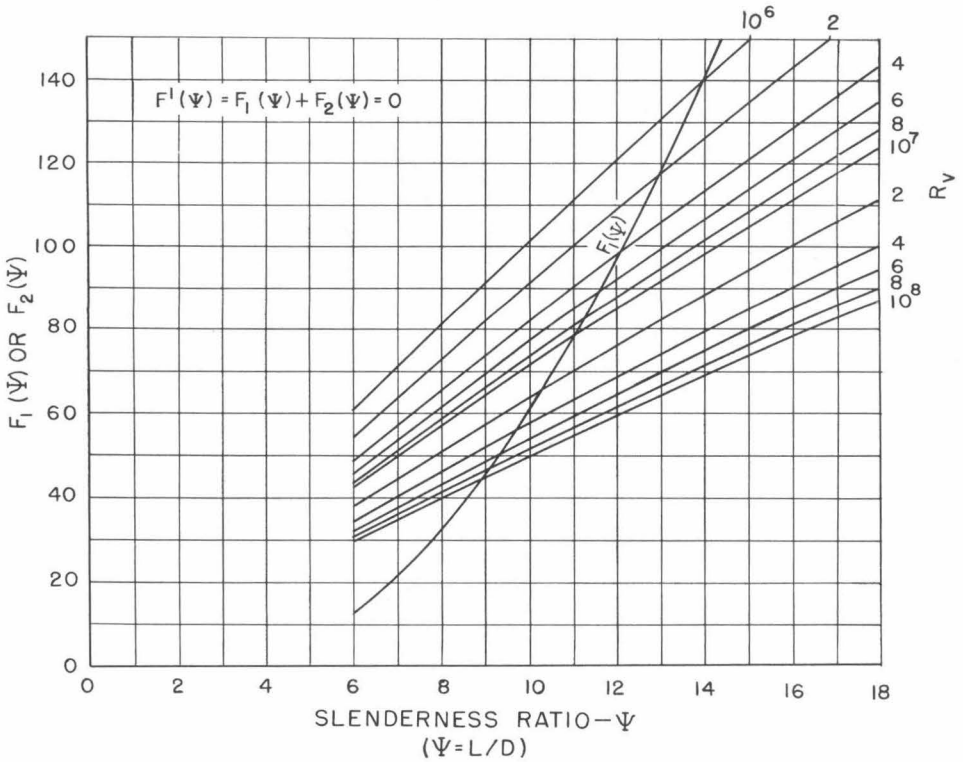

Fig. 25—Effect of Varying Volume Reynolds Number

This chart is based on the MK 13-1 torpedo nose and afterbody. It is important to note that the residual drag curve (Fig. 8) has a steeper slope than the flat plate skin friction curve (see Eq. 15)).

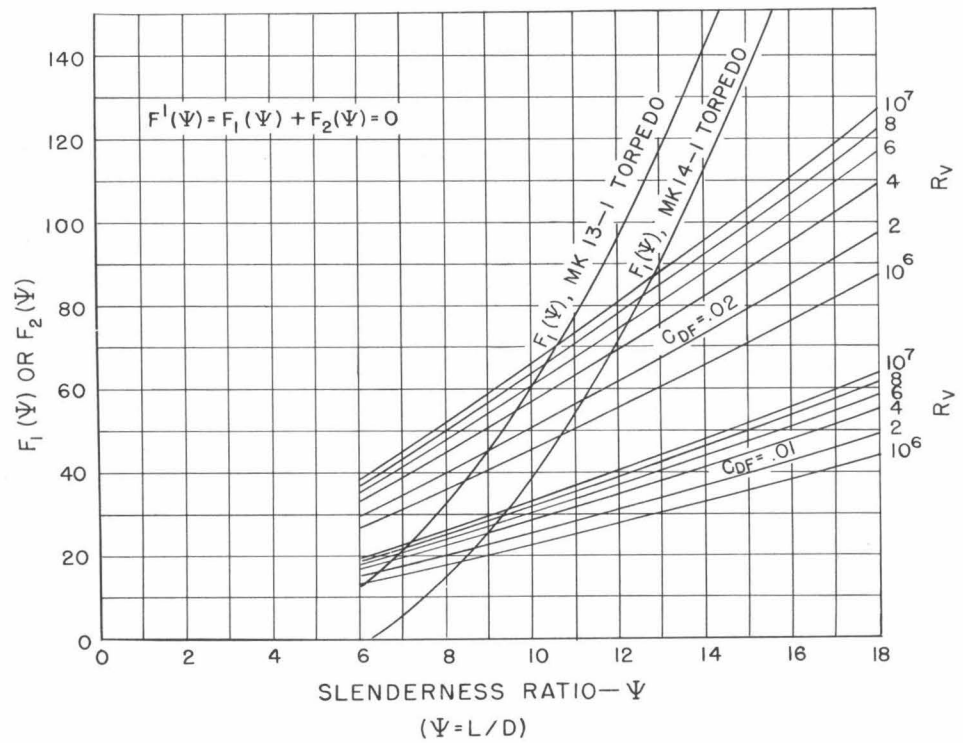

Fig. 26—Effect of Varying Volume Reynolds Number

In this chart it is assumed that the residual drag is constant—two different values being used on the chart.

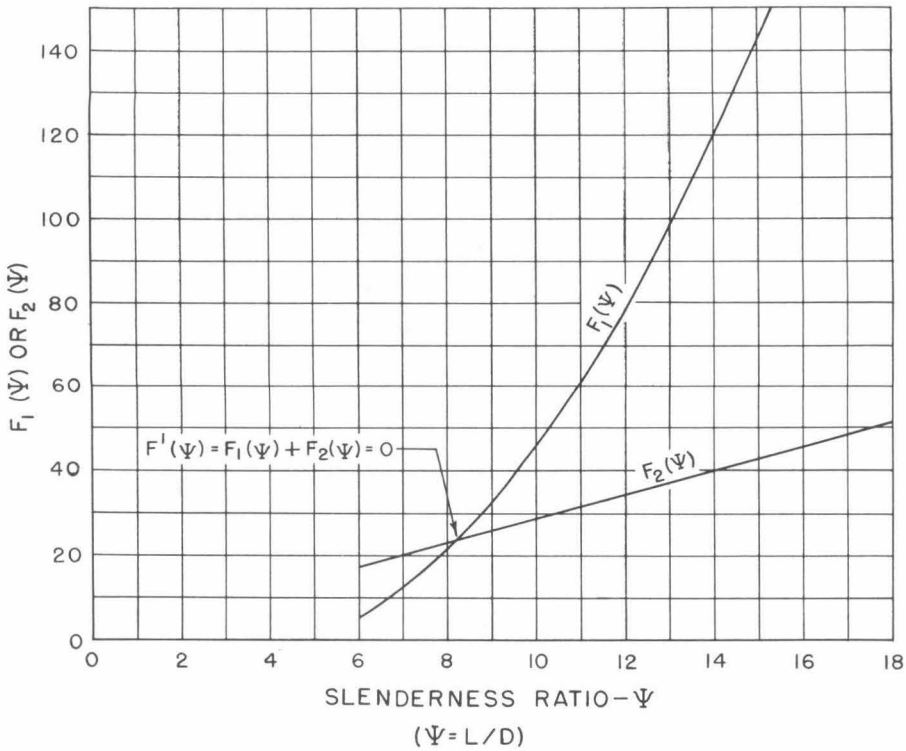

Fig. 27—Maximum Point Chart for MK 13-1 Torpedo and Afterbody Shape

The chart is calculated for an assumed constant residual drag value of 0.013 and an assumed constant skin friction value of 0.00229. This chart gives the maximum point of Fig. 17.

CONSTANT RESIDUAL DRAG AND CONSTANT FRICTIONAL RESISTANCE

Let us assume that the form drag and the frictional resistance coefficients are constant as Reynolds number changes. In this case n and m are zero and C_{DF} equals M, and C_{FP} equals N. Eq. (46) then becomes

$$F_1(\psi) = \psi^2 + [3B - 2Q]\psi - BQ \qquad (50)$$

and Eq. (47) becomes

$$F_2 \qquad F_2(\psi) = -\frac{C_{DF}\,\psi}{2\,C_{FP}} \qquad (51)$$

Evaluation of Eq. (50) for the MK 13-1 shape gives the $F_1(\psi)$ curve in Fig. 27. Using the same values of C_{DF} as in Fig. 17, the result is $F_2(\psi)$ curve in Fig. 27. in Fig. 27.

Thus, we see that for constant residual and frictional resistance, the optimum slenderness ratio is still dependent on their values.

CONCLUSION

A body that has a very low drag coefficient must necessarily have no appendages such as fins, propellers, struts, lugs, etcetera. An example is the Lyon Form A which has a very low form drag coefficient. With no cylindrical midsection, its slenderness ratio is five, and after examining Fig. 24, it is obvious that this figure would be the optimum value. However, to be of practical value, an undersea body must be dynamically stable and maneuverable, for which fins, rudders, and diving planes are required. For propulsion, there are the struts and propellers. Because of these appendages, the residual drag of the body will be appreciable and the surface area will be enlarged. As pointed out in this article, both factors tend to increase the optimum slenderness ratio. To continue the example, consider the same Lyon Form with stabilizing and control surfaces and propellers. With these appendages the optimum slenderness ratio will increase to at least eight or nine.

An examination of a typical characteristic curve (see Fig. 11 or Fig. 13) of a stable body with fins will show that in the region of the maximum point the curve is relatively flat. Therefore, any reasonable variation from the theoretical optimum value will have little practical effect on the velocity of the body. To carry the example one step further, this same body with appendages could be constructed with a slenderness ratio as low as 5 or as high as 13 without reducing the maximum velocity for given power more than two per cent.

Because of practical factors involved in the design of an undersea body, it may be desirable from the designer's point of view to have a relatively large slenderness ratio. This investigation shows that as far as drag per unit volume is concerned, the designer will pay very little if any penalty if he disregards the drag factor and bases his selection of slenderness ratio entirely on such items as tactical requirements of maneuverability, structural design and utilization of internal space.

BIBLIOGRAPHY

1 Doolittle, Harold L., *Tests of the MK 13-1 Torpedo with Various Noses*, HML Report ND 15.4, CIT, Feb. 1, 1945.

2 Davidson, Kenneth S.M., *Resistance and Powering*, Chapter II, Volume II of Principles of Naval Architecture, Rossell and Chapman, 1941.

3 Schoenherr, Karl E., *Resistance of Flat Surfaces Moving Through a Fluid*, Transactions of the Society of Naval Architects and Marine Engineers, Vol. 40, pp. 279-313, 1932.

4 Lyon, Hilda M., *Effect of Turbulence on Drag of Airship Models*, A.R.C. R.&M., No. 1511, 1932.

5 Knapp, Levy, O'Neill, and Brown, *The Hydrodynamics Laboratory of the California Institute of Technology*, Trans. A.S.M.E., pp. 437 to 457, July, 1948.

APPENDIX

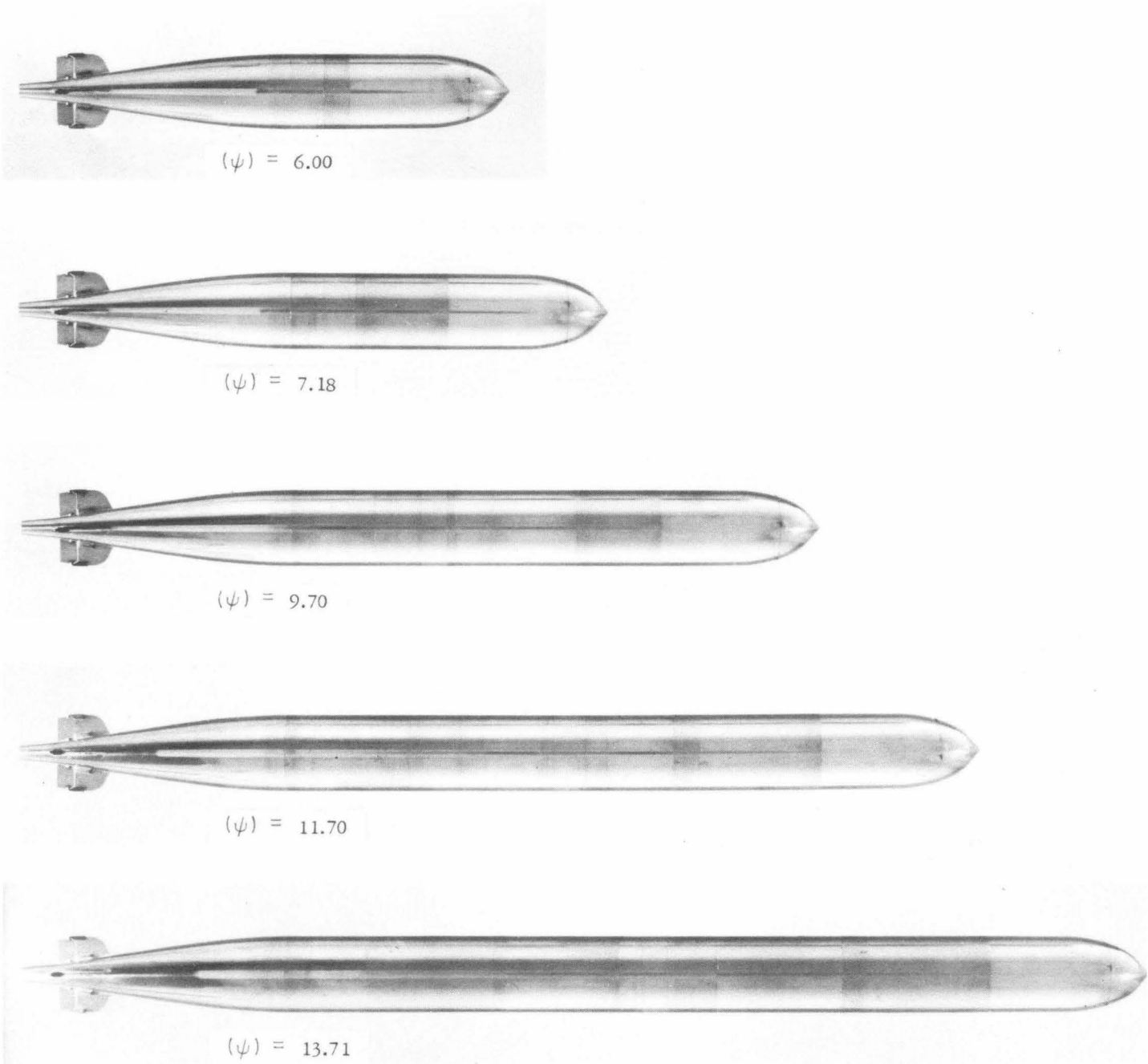

Fig. 28—Slenderness Ratio Study Series

In this series the nose and afterbody are the same as the MK 14-1 torpedo shape. The two-inch diameter model has a spoiler of 0.005" wire one-half diameter from the nose. See Fig. 5 for a typical installation of the model.

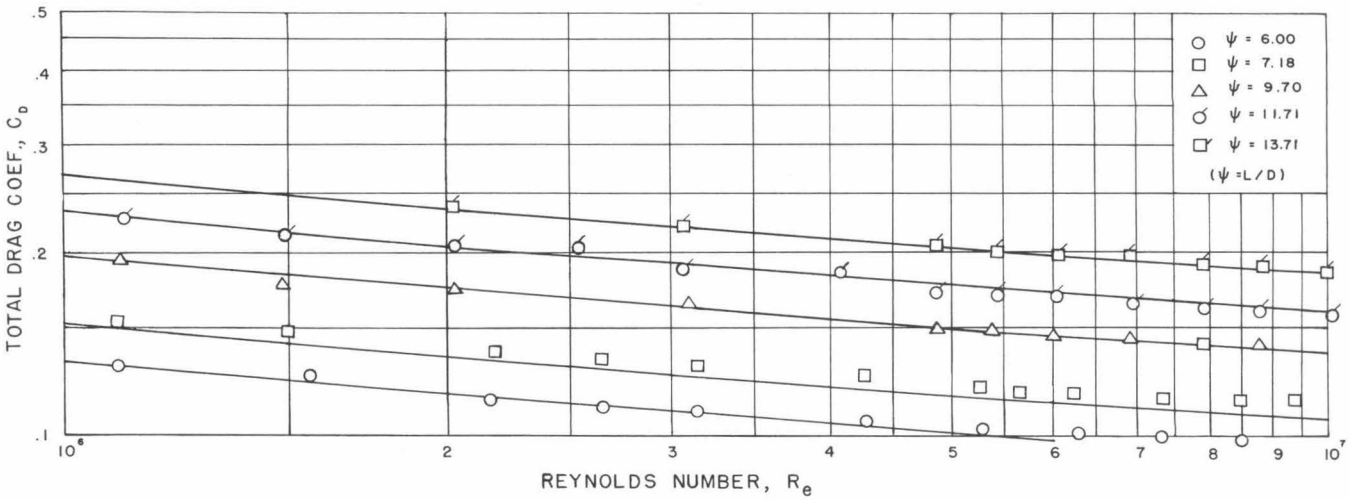

Fig. 29—Total Drag Coefficient vs. Reynolds Number

The experimental points were obtained using the models shown in Fig. 28.

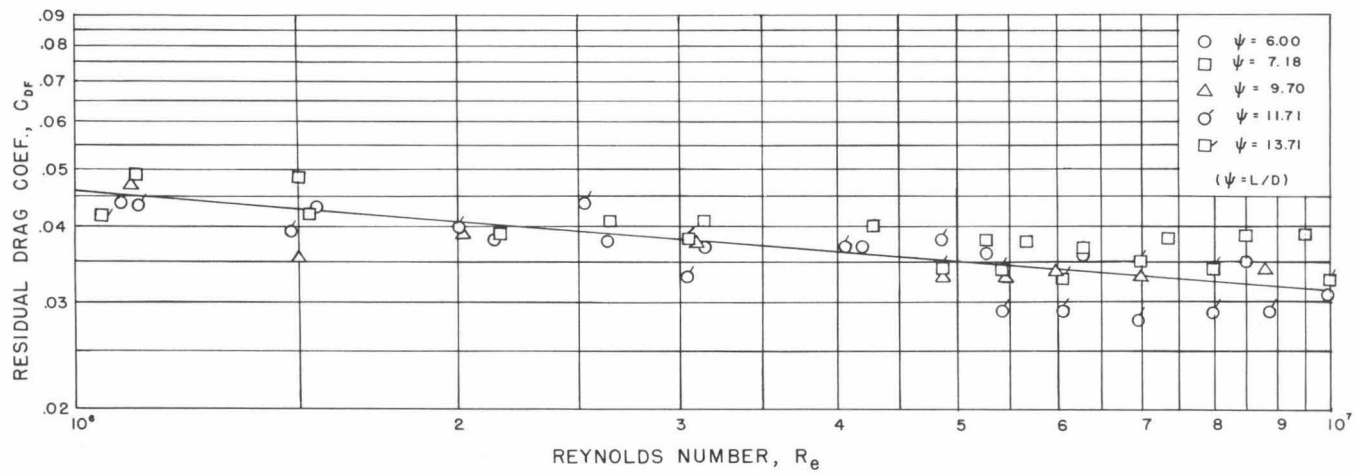

Fig. 30—Residual Drag Coefficient vs. Reynolds Number

The experimental points are calculated by using Eqs. (16) and (17).

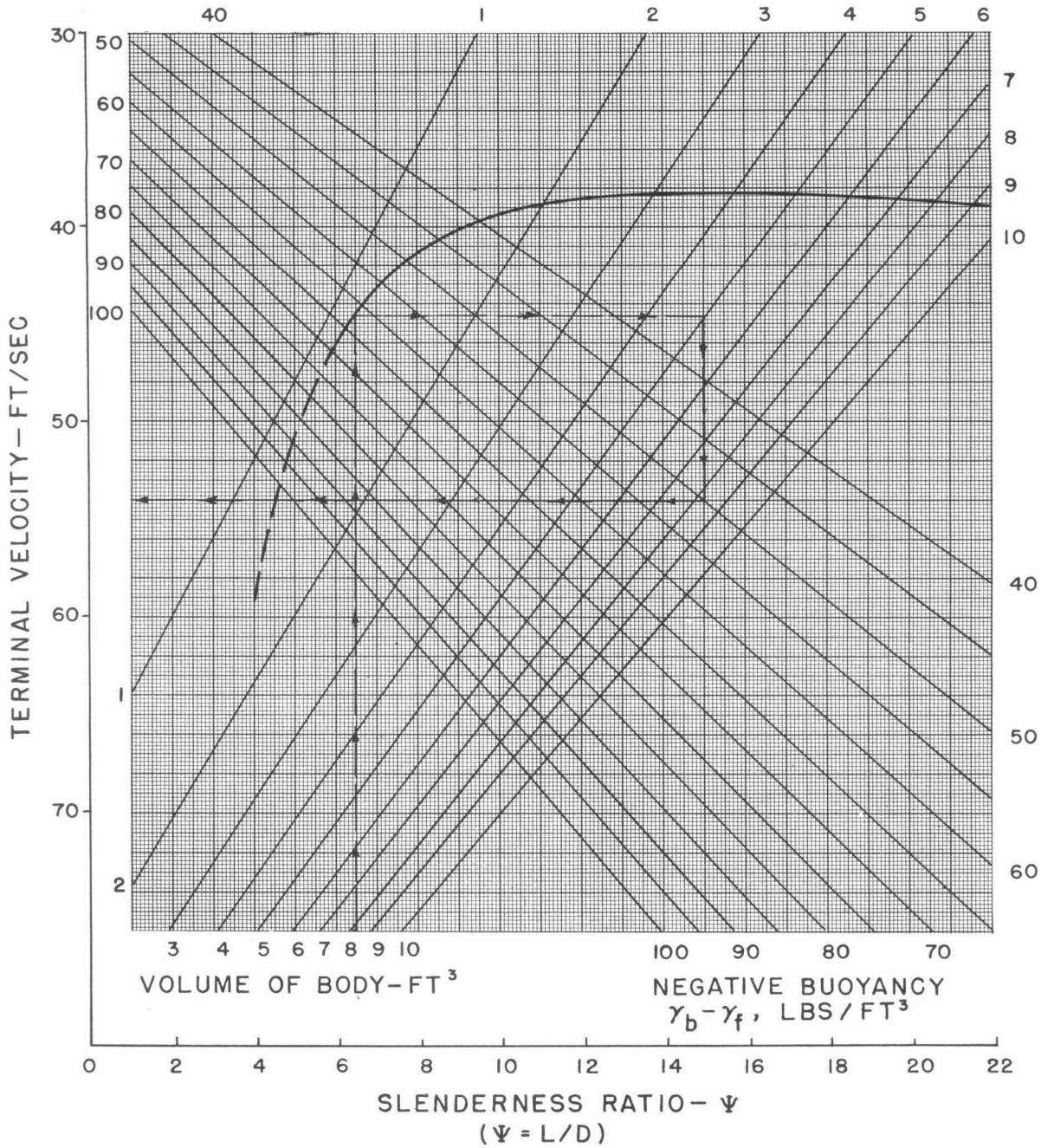

Fig. 31—Sinking Body Velocity Chart for MK 14-1 Torpedo Nose and Afterbody shape

This chart is designed for a free sinking body of a size and velocity range suitable for a depth charge. The characteristic curve is calculated on the basis of the data in Fig. 30 and for an average volume Reynolds number based on the range of velocities and volumes indicated in the chart.

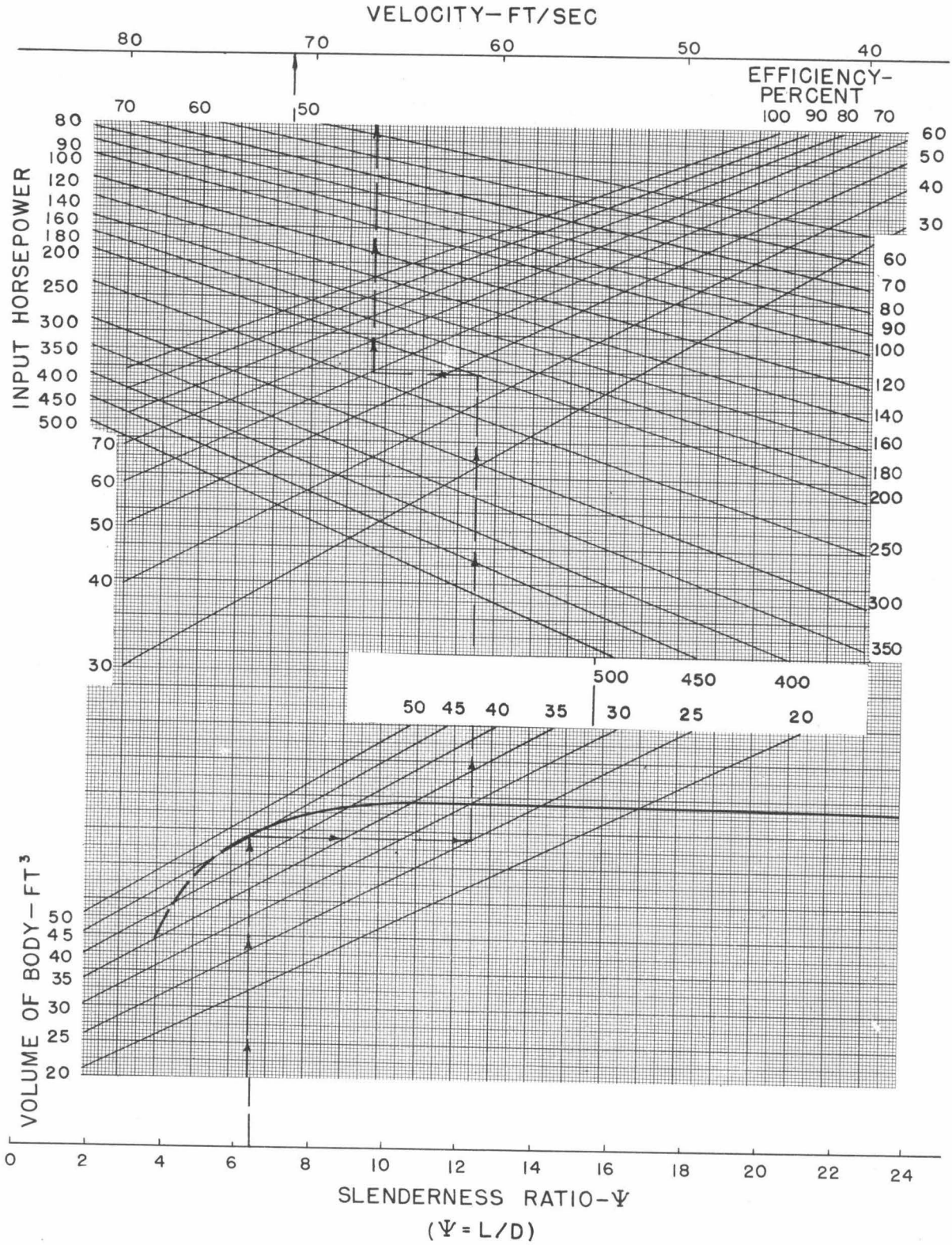

Fig. 32—Horizontally Moving Body Velocity Chart for MK 14-1 Torpedo and Afterbody Shape

This chart is designed for a horizontally moving body in the size and horsepower range of the torpedo. The characteristic curve is calculated on the same basis as the characteristic curve in Fig. 31.

$(\psi) = 6.00$

$(\psi) = 7.18$

$(\psi) = 9.70$

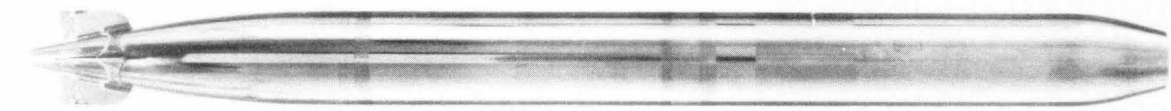

$(\psi) = 11.71$

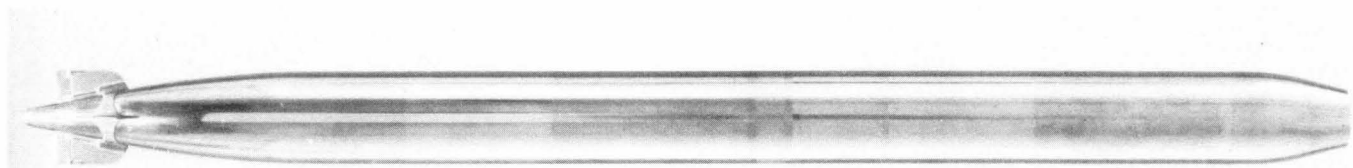

$(\psi) = 13.71$

Fig. 33—Slenderness Ratio Study Series

In this series the nose in a truncated cone faired into the body. The afterbody is the MK 13-1 torpedo shape. See Fig. 5 for a typical installation of the model.

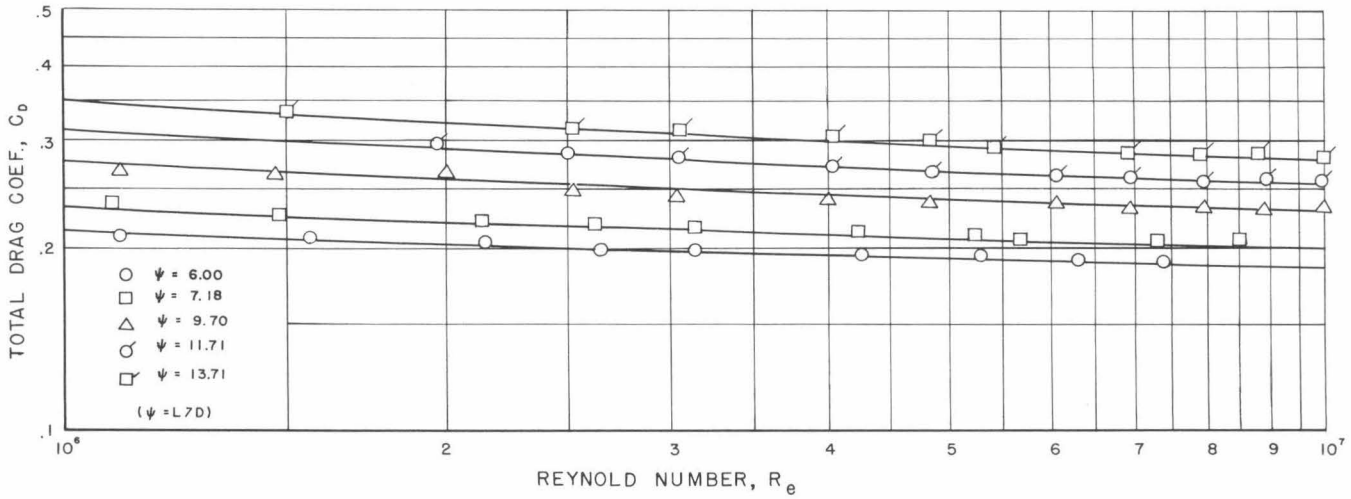

Fig. 34—Total Drag Coefficient vs. Reynolds Number

The experimental points were obtained using the models shown in Fig. 33.

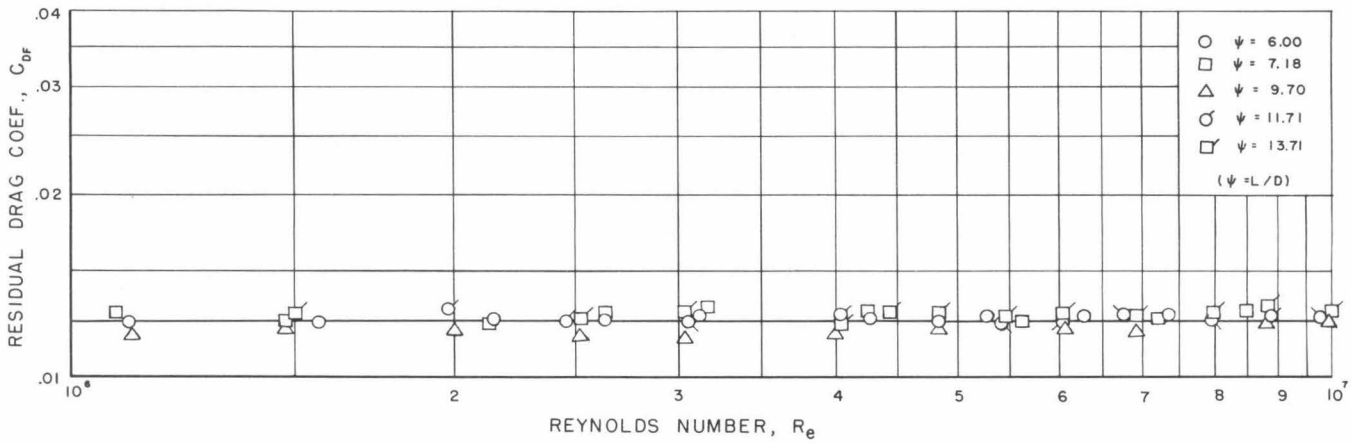

Fig. 35—Residual Drag Coefficient vs. Reynolds Number

The experimental points are calculated by using Eqs. (16) and (17)

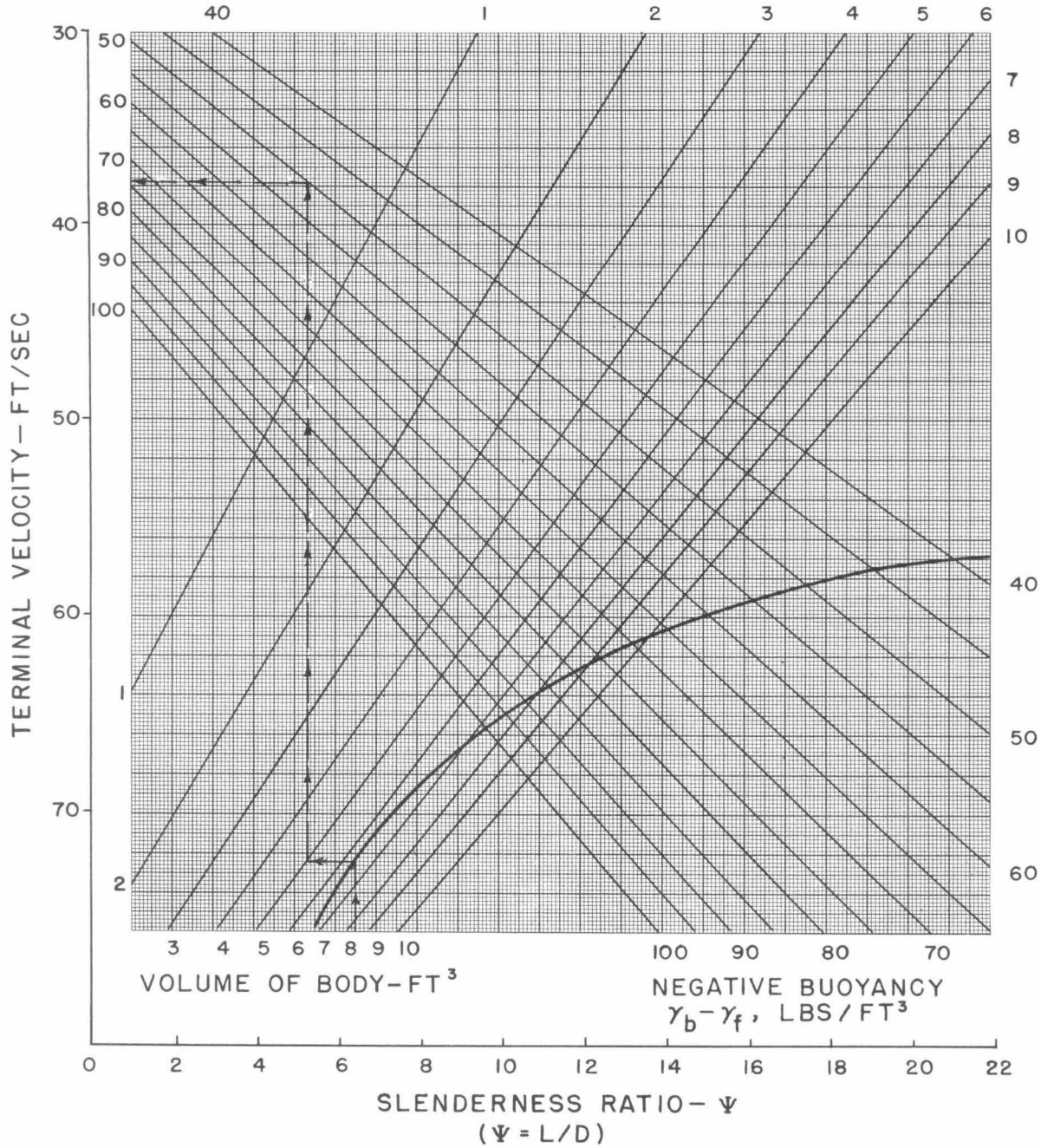

Fig. 36—Sinking Body Velocity Chart for Truncated Nose and MK 13-1 Afterbody Shape

This chart is designed for a free sinking body of a size and velocity range suitable for a depth charge. The characteristic curve is calculated on the basis of the data in Fig. 35 and for an average volume Reynolds number based on the range of velocities and volumes indicated on the chart.

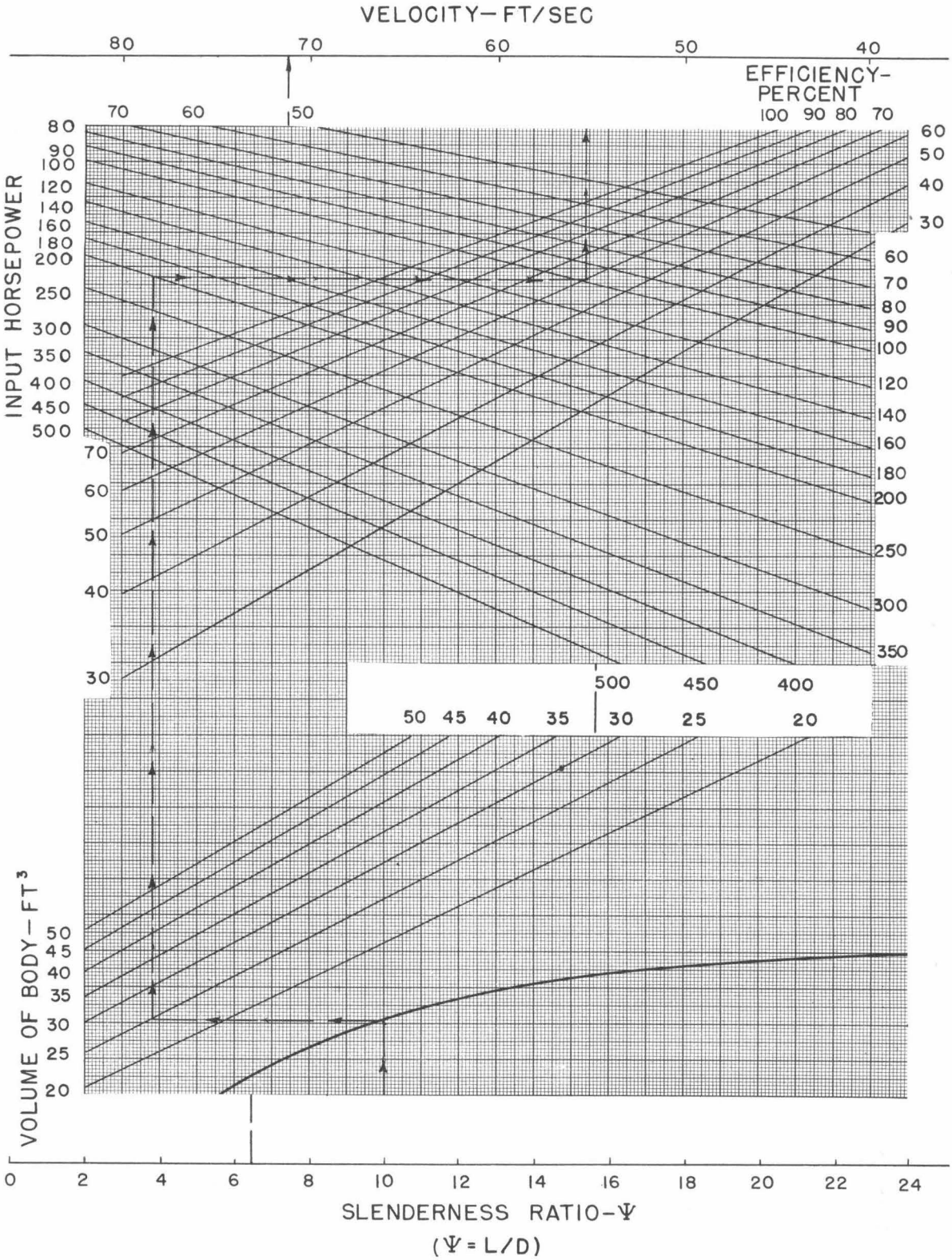

Fig. 37—Horizontally Moving Body Velocity Chart for Truncated Nose and MK 13-1 Afterbody Shape

This chart is designed for a horizontally moving body in the size and horsepower range of the torpedo. The characteristic curve is calculated on the same basis as the characteristic curve in Fig. 36.

DISTRIBUTION LIST

9	Director, Naval Research Laboratory, Washington 25, D.C., Attn: Technical Information Officer
6	Office of Naval Research, Department of the Navy, Washington 25, D.C., Attn: Mechanics Branch (Code 438)
1	Commanding Officer, Branch Office, U.S. Navy, Office of Naval Research, 495 Summer Street, Boston 10, Massachusetts
2	Commanding Officer, Branch Office, U.S. Navy, Office of Naval Research, 50 Church Street, New York 7, N.Y.
1	Commanding Officer, Branch Office, U.S. Navy, Office of Naval Research, 844 North Rush Street, Chicago 11, Illinois
1	Commanding Officer, Branch Office, U.S. Navy, Office of Naval Research, 801 Donahue Street, San Francisco 24, California
2	Commanding Officer, Branch Office, U.S. Navy, Office of Naval Research, 1030 East Green Street, Pasadena 1, California
2	Assistant Naval Attache for Research, U.S. Navy, Office of Naval Research, American Embassy, London, England, Navy 100, F.P.O., New York, N.Y.
1	Chief, Bureau of Ships, Department of the Navy, Washington 25, D.C.
1	Bureau of Ships, Department of the Navy, Washington 25, D.C., Attn: Ship Design Division (Code 410)
1	Bureau of Ships, Department of the Navy, Washington 25, D.C., Attn: Research Division (Code 330)
2	Bureau of Ships, Department of the Navy, Washington 25, D.C., Attn: Preliminary Design (Code 420)
1	Director, David W. Taylor Model Basin, Department of the Navy, Washington 7, D.C.
2	David Taylor Model Basin, Department of the Navy, Washington 7, D.C., Attn: Hydromechanics Division
1	Dr. K.S.M. Davidson, Director, Experimental Towing Tank, Stevens Institute of Technology, Hoboken, New Jersey.
1	Commanding Officer, Office of Naval Research, New York Branch, Bldg. No. 3, Tenth Floor, New York Naval Shipyard, Brooklyn 1, New York